Assessing the Impacts of Simulated Ocean Alkalinity Enhancement on Viability and Growth of Near-Shore Species of Phytoplankton

By

Jessica Oberlander

Submitted in partial fulfilment of the requirements
for the degree of Master of Science

At

Dalhousie University
Halifax, Nova Scotia
April 2023

TABLE OF CONTENTS

LIST OF TABLES

LIST OF FIGURES

ABSTRACT

Over the past 250 years, atmospheric carbon dioxide concentrations have risen steadily from 277 ppm to 405 ppm, leading to the exacerbation of the effects of climate change. As a result, new technologies are being developed to remove carbon from the atmosphere, such as negative emission technologies (NETs). One proposed NET is Ocean Alkalinity Enhancement (OAE), which would mimic the ocean's natural weathering processes and sequester carbon dioxide from the atmosphere. An analysis of published data investigating the effects of elevated pH on phytoplankton growth rate and experimental assessment of pH dependence of viability and growth rate was used to assess the potential impacts of OAE. Viability was assessed with a modified Serial Dilution Culture – Most Probable Number assay. Chlorophyll a fluorescence was used to test for changes in growth rates and photosynthetic competence. The results from this study suggest that there will be no significant impact on the viability or growth rates of *Thalassiosira pseudonana* or *Pavlova lutheri* with short-term (10 minute) exposure to elevated pH. However, when long-term (days) exposure occurs there is a significant decrease in growth rates with elevated pH. Short-term exposure is anticipated to more closely mirror the natural systems in which OAE will be implemented because of system flushing and replenishment of nutrients. These preliminary findings suggest that there will be little to no impact on a variety of taxonomic groups of phytoplankton when OAE occurs in naturally flushed systems.

LIST OF ABBREVIATIONS AND SYMBOLS USED

Abbreviation/Symbol	Definition
CDR	Carbon Dioxide Removal
CCM	Carbon Concentrating Mechanism
MRV	Measurement, Reporting, and Validation
NETs	Negative Emissions Technologies
OAE	Ocean Alkalinity Enhancement
SDC–MPN	Serial Dilution Culture – Most Probable Number
CO_2	Carbon dioxide
DIC	Dissolved Inorganic Carbon
OH^-	Hydroxide
HCl	Hydrochloric acid
HCO_3^-	Bicarbonate
$Mg(OH)_2$	Magnesium hydroxide
NaOH	Sodium hydroxide
$NaHCO_3$	Sodium bicarbonate
LLD_F	Lower limit of detection for fluorescence
RV	Relative viability (dimensionless)
MPN_{med}	Median of tabulated value of MPN for calculable tube scores
N_{viable}	Concentration of viable cells
PSII	Photosystem II
t_{end}	Time to end the SDC–MPN assay
t_{lag}	Time of lag phase
t_{stat}	Time to stationary phase
Y	5 generation buffer
α	Coefficient to partition the biphasic response
b	Curvature parameter for Bannister model
$cells_{init}$	Initial concentration of cells

$cells_{fin}$	Final concentration of cells
F_{init}	Initial fluorescence value from growth curve
F_{fin}	Final fluorescence value from growth curve
F_0	Minimum fluorescence from induction curve
F_m	Maximum fluorescence from induction curve
F_v	Variable fluorescence from induction curve
k, k_1, k_2	Slope of biphasic or 1st order kinetics models
pH_{Th}	Threshold pH
F_v/F_m	Maximum quantum yield of photochemistry in PSII (dimensionless)
μ	Growth rate (d^{-1})
μ_{max}	Maximum growth rate (d^{-1})
CV	Coefficient of variation
CI	Confidence Interval
ppm	Parts per million
°C	Degrees in Celsius
≤	Less than or equal to
>	Greater than
%	Percent
c.	About

ACKNOWLEDGEMENTS

I would like to start by thanking my supervisor, Dr. Hugh MacIntyre because without his support and guidance this research would not have been possible. From the many, many zoom meetings to finally having in-person meetings to pestering him with questions as I wrote this thesis, he has always responded with a smile and a thought-provoking response, and for that I will forever be grateful. Through the bumpy journey that has been my degree, he has been like a lighthouse guiding me to the shore. I am so incredibly lucky to have been able to learn from him and am thankful for his invaluable experience in shaping me into the scientist I am today. I would also like to thank the members of my supervisory committee, Dr. Carolyn Buchwald and Dr. Christopher Algar, for their insight and advice while completing my degree.

Of course, none of this work would have been possible without the help of the MAPEL lab members both past and present. I would specifically like to thank our lab manager Cat London, who has helped not only with guiding my lab work but also my own personal growth. To my lab kids, Mikaela Ermanovics and Mackenzie Burke, who not only helped me in the completion of lab work but also taught me how to be a mentor, thank you. I would like to thank the co-op students who have come through the lab over the past two and a half years, helping with culturing and analytical work: Jacqueline Lossing, Jensen Keltie, Ryan Molin, Griffin Finkbeiner, Ainhoa Fournier, Meghan Oliver, Madeleine Platt, and Rori Mulholland, as well as our lab technicians Julia Cantelo and Rose Latimer. And to my fellow lab graduate students, Tatyana Bouffard-Martel, Marie Egert, and Laura Figueira Garcia, thank you for supporting me when the going got tough. I could not have completed this degree without any of you.

Lastly, I would like to thank my friends and family for all of their love and support over this journey. In particular I would like to thank my DOSA friends Jenna Hare, Maddy Healey,

Katie Frame, Wendy Muraoka, and my fellow DOSA Exec members for their friendship and always being available to chat. Thank you to my friends from afar, Jeri Sloan and Hannah Meadows, for answering my facetime calls and listening to my science chats even though they didn't know what I was talking about half the time. Thank you to Sofya Pesternikova for being one of my first friends in Halifax and being so supportive through my whole degree. To my parents, thank you most of all. Without their love and support it would not have been possible for me to move countries in the middle of a pandemic and I might never have started graduate school. Finally, a thank you to any and everyone who has helped me along the way big or small, who may not have been mentioned here. When they say it takes a village, they really mean it and so many have helped me along this journey.

This project was supported by Grant CRDPJ 520352-17 from the Natural Sciences and Engineering Research Council of Canada and by donations from the ClimateWorks Foundation and the Thistledown Foundation.

CHAPTER 1

INTRODUCTION

1.1 Background

The issue of climate change has become one of the most pressing problems facing us as a society. Atmospheric carbon dioxide concentrations have been steadily increasing for the past 250 years, with current concentrations of approximately 405 ppm (Dlugokencky and Tans, 2018). This increase is a problem because greater concentrations of CO_2 lead to an increase in the greenhouse effect, warmer temperatures, and increased ocean acidification (Zhong & Haigh, 2013; IPCC, 2018). While environmental impacts will be most prevalent, human-related issues will also rise, including limited water availability and biome shifts (UNESCO, 2011; IPCC, 2018). Overall, the issue of climate change needs to be addressed quickly and with care taken to ensure little to no negative impacts.

Ocean acidification is one of the primary impacts of climate change on the ocean (IPCC, 2018). The associated decrease in pH has the possibility of placing many marine organisms, including phytoplankton under environmental stress. Phytoplankton growth rates have been documented as being sensitive to changes in pH, with deviations from the norm in either direction resulting in negative impacts (Hansen, 2002). However, certain phytoplankton, notably the diatom *Phaeodactylum tricornutum*, are able to tolerate a pH above nine and below seven without reducing their growth rate to zero (Berge et al., 2010; Hansen, 2002). A decrease in growth rate could be due to a change in vitality (*i.e.,* reduced metabolic competence), or possibly because of a reduction in viability in a fraction of the population. This distinction between vital and viable is critical since vitality refers to whether an organism is alive, and

viability refers to an organism's ability to reproduce; a cell can still be classified as vital without being viable (Blatchley III et al., 2018).

Increasing atmospheric concentrations of CO_2 and temperature have led to the creation of the Paris Agreement between multiple nations, with the goal being to keep the global average increase in temperature below 2 ℃ (*United Nations Framework Convention on Climate Change*, 2015). However, to reach this goal, not only will carbon emissions need to be reduced, but carbon will need to be removed from the atmosphere. Implementation of Negative Emissions Technologies (NETs), which would remove carbon dioxide from the atmosphere to meet the goal of a maximum increase of 2 ℃, are essential (Minx et al., 2018). There are a multitude of NETs that have been proposed, both land- and ocean-based, that have yielded encouraging results. These include ocean-based renewable energy, restoration of coastal vegetation, ocean fertilization, artificial downwelling, biomass burial, Ocean Alkalinity Enhancement (OAE), and many more (Keller et al., 2018; Magnan et al., 2018.). Ocean Alkalinity Enhancement has the potential to be one of the most effective NETs, as the ocean has already absorbed c. 40% of the anthropogenic carbon from the atmosphere (Renforth & Henderson, 2017). Ocean Alkalinity Enhancement would also aid in reducing the impacts of ocean acidification and the resulting negative effects on marine organisms. The implementation of OAE involves enhancing the carbon uptake by mimicking natural weathering processes through the addition of alkalinity, reducing ocean acidification and increasing buffering capacity (Lenton et al., 2018).

Planetary Technologies has proposed a form of OAE as a Carbon Dioxide Removal (CDR) technology. Their method uses mine tailings that have been exposed to an electrochemical process to purify them before being released into the ocean (www.planetarytech.com/technology/). The mine tailings are put through a process called heap

leaching, in which the tailings are piled together, and a leaching reagent, usually an acid, is poured over the top to strip out any metals (Ghorbani et al., 2015). The leached solution containing the metals is acidic, and great care must be taken when handling it for metal extraction (Ghorbani et al., 2015). One of the key metals extracted from heap leaching is magnesium (Mg). The extracted Mg is then exposed to water electrolysis, where water molecules are split into H^+ and OH^- ions, forming magnesium hydroxide ($Mg(OH)_2$) and other nontoxic byproducts (Rau et al., 2018). The $Mg(OH)_2$ can then be released into coastal oceans through waste pipes, such as from power plants, to aid in sequestering atmospheric carbon, ultimately transporting it into the deep sea (Rau et al., 2018). There has not yet been any quantification on the amount of carbon that can be captured using this method, and the volume of $Mg(OH)_2$ that will be used has also not been defined. While these processes are not entirely new, combining them in this fashion to sequester carbon is innovative; however, it is crucial to confirm that there will be little to no impact on ocean biota, specifically phytoplankton, as they are the base of marine food webs.

The first step to determine how OAE might affect phytoplankton is to examine the physiological responses in cultures. Reductions in photosynthetic competence can inhibit phytoplankton growth rates while still allowing the cells to remain fully viable. Previous experiments suggest that there is a threshold value of alkalization, above which the physiological functions are impaired and the growth rate is reduced (Berge et al., 2010, 2012; Hansen, 2002; Hansen et al., 2007). Contextualizing how these possible impacts relate to pH in situ in different coastal regions where OAE is likely to be tested is vital for its acceptance. The combination of changes to physiological parameters, data from previous studies, and data on the natural

variations in pH gives context for the range of OAE likely to be tolerated by phytoplankton, and thus a starting point for investigating the impacts on viability.

The method used to test for the impact of alkalization on phytoplankton viability in this thesis is the Serial Dilution Culture – Most Probable Number (SDC–MPN) assay (McCrady, 1915; USEPA, 2010). This method is based on monitoring a dilution series for an extended period, scoring the replicate samples for growth versus no growth, and using the scores to calculate the concentration of viable organisms in the original, untreated sample (McCrady, 1915). The SDC–MPN method was initially developed to assay viability in bacteria (McCrady, 1915), but has since been adapted for phytoplankton (Allen, 1919; Throndsen, 1978; MacIntyre et al., 2018; MacIntyre et al., 2019). There are, however, drawbacks associated with the method, including the length of experiments, the human effort needed to complete a single experiment, and concerns regarding the reliability of application to mixed populations (Cullen & MacIntyre, 2016; MacIntyre et al., 2018).

The primary assumptions of the SDC–MPN assay are that the organisms have been randomly distributed in each dilution and that their growth can be detected reliably (McCrady, 1915). The first assumption can be satisfied by ensuring that cultures are well-mixed before beginning the dilutions and that each sample is homogenous, with the caveat that aggregation will still bias the outcome. The second assumption requires a reliable means of measuring growth. The assay adopted for phytoplankton is generally completed in borosilicate glass tubes, and growth is measured using fluorescence as a proxy, but this requires monitoring a large number of individual cultures for extended periods (MacIntyre et al., 2018). In order to increase throughput, the SDC–MPN assay was modified to use 24-well polystyrene cell culture plates and a BioTek Synergy 4 Hybrid Multi-Mode Microplate Reader (Model S4MLFTAD).

This modification allows for all tiers of dilution to be monitored simultaneously, decreasing the time needed for culture monitoring. Nevertheless, validation of the modification was needed before any results could be accepted as accurate and precise.

1.2 Goals and Objectives

This research assessed the impact of simulated Ocean Alkalinity Enhancement on species of phytoplankton characteristic of the spring and fall blooms in Bedford Basin, Nova Scotia, Canada. This was accomplished by the following three objectives:

1. Examining natural variations in pH and previously published data on phytoplankton responses to changes in pH,
2. Verifying the validity of a modified SDC-MPN assay; and
3. Using the modified assay to assess how the viability of different lineages of phytoplankton respond to increased pH.

Previously published data on the effect of elevated pH on growth rates is examined, along with seasonal pH values from coastal Atlantic monitoring sites in Chapter 2. The methods testing associated with verifying the validity of a modified SDC–MPN assay is presented in Chapter 3. This includes the validation of control treatments in plates with control treatments in glass tubes, testing different phytoplankton lineages, and ensuring valid results could be replicated. The responses of *Thalassiosira pesudonana* and *Pavlova lutheri* to elevated pH are presented in Chapter 4. The responses are based on the modified SDC–MPN assay and include dose-response curves for viability and for indices of photosynthetic competence. The implications of the results are then discussed. The findings are then summarized in Chapter 5.

CHAPTER 2

EXAMINING PHYTOPLANKTON RESPONSES TO pH IN TERMS OF OCEAN ALKALINITY ENHANCEMENT

2.1 Abstract

The ocean is one of the most important environments on earth, and provides many valuable services such as food, oxygen, and climate regulation. However, an increasing carbon content due to anthropogenic release is leading to a decrease in the average pH and changes in the primary speciation of carbon. These changes can have major repercussions on the growth of phytoplankton. Published data on the impact of elevated pH on different lineages of phytoplankton was digitized and modeled to determine a threshold pH above which a decrease in growth rates could be measured. Examining the threshold pH values for six different taxonomic groups determined that there is a statistical difference in the response between groups, with the major difference being between dinoflagellates and all others. Further examination into the responses of dinoflagellates reveals that there is large variability even within the single species of *Heterocapsa triquetra*, which accounts for almost half of the data points in the dinoflagellate group. When examining the difference in threshold response between culturing types (semi-continuous and batch) for the same strains of *Ceratium* there is no statistical difference, likely because the cultures were able to acclimate to the conditions. While there is still much more to investigate, namely attempting to disentangling the effects of pH, DIC and light attenuation in batch cultures, the analysis presented here provides a first-order analysis of the potential impact of implementing OAE on a larger scale.

2.2 Introduction

The ocean makes up c. 70% of the planet's total surface area and produces ample food for a vast number of organisms in varied environments while having a pivotal role in climate regulation by storing heat and atmospheric gases (Galland et al., 2012). However, increasing global temperatures, ocean acidification, and sea-level rise are climate change-associated threats to the ecosystem services that the ocean currently provides (Gattuso, 2018). The ocean's ability to act as a carbon sink and buffer the changes occurring in the atmosphere is being pushed to its limit, and is quickly becoming overburdened by the excess carbon emitted into the atmosphere (Galland et al., 2012). The increase in the uptake of carbon dioxide is causing a shift in the ocean's chemical equilibrium, leading to a decrease in the overall pH and a reduction in the concentration of carbonate (Lenton et al., 2018). As this process continues, the ocean's buffering capacity will decrease and cause ocean acidification to increase even faster (Lenton et al., 2018), placing marine ecosystems at a greater risk for degradation. As a result, Negative Emission Technologies (NETs) are being created to remove carbon from the atmosphere and sequester it elsewhere for long timescales. A promising NET, Ocean Alkalinity Enhancement (OAE), would enhance the ocean's natural weathering processes and store carbon in the form of bicarbonate. This is completed through the addition of hydroxide to coastal oceans, which is able to react with carbon dioxide in the atmosphere, to form bicarbonate, but this can cause changes in the pH and dominant carbon species.

The pH scale is used to describe how basic or acidic a solution is and its measurement is useful in detecting ocean acidification events or testing the buffering capacity of the ocean. pH is defined as $-\log_{10}[H^+]$, where $[H^+]$ is the hydrogen ion concentration in mol L^{-1}, with acidic solutions having a greater concentration of H^+ (pH <7) and basic solutions containing a greater

concentration of OH^- (pH≥7; Flowers et al., 2019). The average pH of the ocean is about 8.2, meaning that there is a slightly greater concentration of OH^- ions than H^+ ions. The relationship

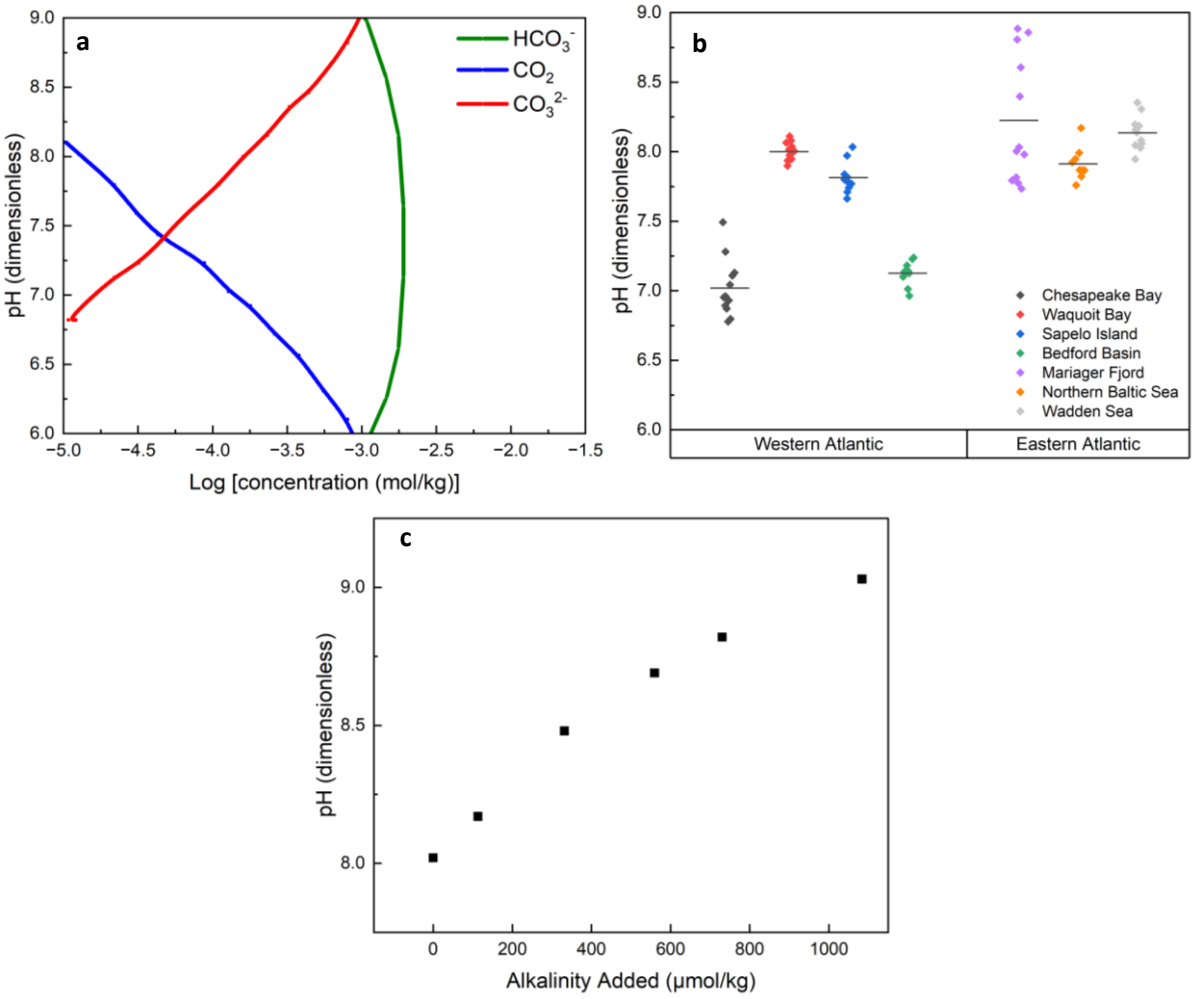

Figure 1: (a) Bjerrum plot displaying the pH-dependence in carbon speciation scaled from pH 6 to pH 9. (b) Time-series data of pH from monitoring sites in the margins of the western and eastern North Atlantic Ocean. Each data point is a monthly average based on published time-series data, and each site contains at least one year's worth of averaged data. For each site, the horizontal bar is the annual mean value. (c) The relationship between additions of alkalinity and pH in seawater from Ketch Harbour, NS (salinity c. 30 PSU).

between these two ions is important for understanding how carbon speciation could change in the ocean with increased acidification, and for understanding what the response will be if OH^- is added in large quantities to act as a CDR technology.

Figure 1a displays a partial Bjerrum plot showing the pH-dependent speciation of dissolved inorganic carbon (CO_2, HCO_3^-, and CO_3^{2-}). As excess carbon is released into the atmosphere and then taken up by the ocean, the pH will decrease as a result of the increasing concentration of CO_2 and decreasing the concentration of carbonate and the ocean's buffering capacity (Lenton et al., 2018). If hydroxide ions were added into the ocean, the pH would rise and the concentration of carbonate ions would increase.

Figure 1b summarizes time series of pH measurements collected from estuarine and coastal locations in the western and eastern North Atlantic Ocean. The wide range in mean annual pH shows how varied the carbon speciation (Figure 1a) can be between different ecosystems and is a consideration where altering the system by Ocean Alkalinity Enhancement (OAE). Figure 1c displays how pH changed with increasing additions of alkalinity simulating OAE in water from Ketch Harbour, NS. This provides context for how OAE conducted with different alkalinity additions (*i.e.*, initial hydroxide concentrations) could alter the pH and carbon speciation in addition to the variation in natural set points illustrated for the locations examined in Figure 1b.

It is important to understand how changes in pH and carbon speciation with OAE could impact marine organisms, notably phytoplankton that are the base of most marine food webs. All phytoplankton rely on ribulose-1,5-bisphosphate carboxylase/oxygenase (Rubisco) in the Calvin cycle to assimilate carbon within the cell (Raven et al., 2017). However, the reaction is generally undersaturated since the current concentration of CO_2 available for phytoplankton (*i.e.* dissolved

in the ocean) is only about 10 mmol m^{-3} (Raven et al., 2017) while Rubisco's half saturation concentration is 105 – 290 mmol/m^3 (Jordan and Ogren, 1981; Tcherkez et al., 2006; Badger and Bek, 2008; Shih et al., 2016). The low concentration is because the average pH of seawater causes the primary speciation of inorganic carbon to be pushed towards HCO_3^- instead of CO_2 (Figure 1a). Nonetheless, the cellular requirements for CO_2 remain high in phytoplankton and most have adapted to the limitation by using carbon concentrating mechanisms (CCMs). The CCMs allow cells to either take up HCO_3^- from the surrounding environment through anion exchange (*i.e.*, hydroxide pumps) followed by conversion of HCO_3^- to CO_2 by carbonic anhydrase, or to actively transport of CO_2 across the cell membrane for use by Rubisco (Colman et al., 2002; Nimer et al., 1997). Both of these processes, the CCM and carbonic anhydrase, are likely to be vulnerable to changes in pH as they rely on a pH gradient to function. Further, not all species can actively transport HCO_3^- into the cell or have carbonic anhydrase. Thus, there is a potential for selective disruption of the community and an increase in the metabolic costs of CCM use, leading to an overall reduction in community growth rates or to shifts within the dominant organisms with elevated pH.

The literature suggests that there is a relationship between pH and growth rates for photosynthetic phytoplankton. The relationship could potentially be due to less efficient operation of the CCMs and carbonic anhydrase outside of the ideal range. Species of diatoms, prymnesiophytes, raphidophytes, cryptophytes, and chlorophytes all display a reduction in growth as the pH is elevated (Berge et al., 2010; Liu et al., 2007; Lundholm et al., 2004). Heterotrophic phytoplankton can also be impacted by pH changes (Berge et al., 2012; Hansen, 2002; Hansen et al., 2007; Nielsen et al., 2007). This is of note since heterotrophs consume prey and do not utilize free carbon to conduct photosynthesis. The published data, specifically on

Gyrodinium dominans, shows a clear threshold for tolerance to pH, above which there is a decline in growth rates (Pedersen & Hansen, 2003). A pH threshold suggests that there are other internal functions, other than photosynthesis, that are negatively impacted by an increase in pH. Hansen et al. (2007) note that one possibility could be that high pHs can decrease the solubility of necessary micronutrients. More likely is that altering the extracellular pH will lead to an increase in intracellular pH, thus having negative effects on vital enzymatic processes (Hansen et al., 2007).

The majority of the work examining the impacts of alkalization has been completed using laboratory cultures which is the best method of data collection without risking environmental contamination. Hansen and co-workers (Hansen, 2002; Lundholm et al., 2004; Hansen et al,. 2007; Schmidt & Hansen, 2001; Møgelhøj et al., 2006; Nielsen et al., 2007;

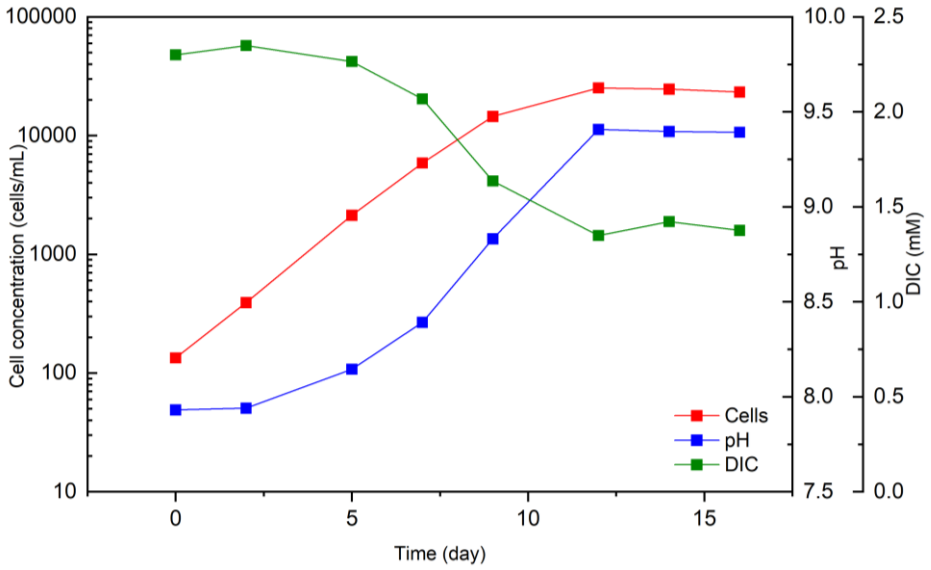

Figure 2: Data digitized from Figure 2b in Hansen et al. (2007) showing trends in cell concentration, pH, and DIC in a batch culture of the dinoflagellate *Heterocapsa triquetra*. Note the simultaneous decrease in DIC, increase in pH, and onset of stationary phase in the later part of the experiment.

Berge et al., 2012; Søgaard et al., 2011; Søderberg & Hansen, 2007) are responsible for most of the work around the impacts of elevated pH on phytoplankton, being motivated by the high pH found in Mariager Fjord due to eutrophication and DIC drawdown. This work could be extrapolated to the simulated effects of OAE since conditions of high nitrogen and phosphorus relative to DIC and elevated pH are comparable to the proposed use of waste-water discharges for OAE. Assessment on the effect of pH on growth by Hansen, and others, has largely been conducted in batch cultures but there are inevitably multiple covarying factors.

Figure 2 shows a time-course of biomass accumulation and the simultaneous draw-down of DIC and increase in pH in a batch culture, using data digitized from Figure 2b in Hansen et al. (2007). It illustrates why pH is not the only factor that should be considered when examining changes in phytoplankton growth in batch cultures. The increase in pH coincides with the decrease in DIC and both reach a plateau on the same day, as the culture enters stationary phase. This suggests that both pH and DIC could be limiting factors for growth. In this instance, nitrogen and phosphorus have been provided in excess (Hansen et al., 2007) so carbon availability is more likely to be limiting to growth than pH. These macronutrients would also become less available as biomass increases and higher C:N:P ratios in the media could also be limiting for growth in an elevated pH scenario. Another possible limitation for growth here could be light attenuation. As a batch culture grows the density of the culture increases, and less light is readily available for cells that are growing away from the wall of the culture vessel (MacIntyre & Cullen, 2005). All these limitations only occur in batch cultures however, and a culture grown with high-pH media in a semi-continuous culture would not experience the same issues. This is because nutrients would continuously be replenished and the culture would be less likely to reach a density at which light attenuation would become a problem. Although the growth-dependent

increase in pH would not be observed since the culture would be maintained at relatively low concentration and in exponential phase growth, pH can be manipulated as an experimental variable. This approach has been employed in a relatively small number of studies (*i.e.*, Søderberg & Hansen, 2007).

It can be difficult to disentangle the relationship between pH and the availability of DIC, other nutrients, and light when examining the impact of hydroxide additions on phytoplankton. Examining each in both laboratory and natural environments, as well as batch and semi-continuous cultures, will help to understand the potential impacts of OAE on phytoplankton. The first step to tackling this hurdle is investigating more closely the response of elevated pH on a variety of phytoplankton lineages to determine which strains are more sensitive than others.

2.3 Methods

2.3.1 Literature Review and Data Digitization

A literature review was conducted to collate data from various studies that have used either batch or semi-continuous cultures to assess the effect of elevated pH on growth rates of phytoplankton. Using the search engine Web of Science and the search terms “phytoplankton AND (alkalinization OR "high pH")” yielded 128 results for articles that discuss this topic; however, many of the articles focus on lake systems as opposed to oceanic systems and species. Thus, other criteria for use in the review included species/strains of phytoplankton indicative of marine systems, as well as differences in growth media, irradiances, or temperatures. The majority of papers collected from this review came from Hansen and colleagues, as they utilized consistent approaches throughout their experiments and indicated nutrient stoichiometry which

was designed to ensure DIC limitation as opposed to nitrogen or phosphorus. This allowed for a wide range of conditions to be compared when determining the potential trends of the change in pH on the growth of different phytoplankton. A complete breakdown of article categorization is given in Supplementary Table A.1.

The data in each study was digitized using OriginPro 2022b (9.9.5.167, Learning Edition) to test for the range of responses in growth rate to pH using a common model. Digitization included importing graphs from the published literature into OriginPro, where data points were then manually selected by choosing the middle of each point. The axis value ranges were imputed and the values corresponding to the selected data points were determined by the software. To determine the error associated with the digitization, random numbers were generated and plotted against a linear series. The plot was then digitized using OriginPro 2022b and the error in the y-axis values was calculated from the original random numbers. The root mean square error (RMSE) for digitization is 0.4% of the maximum of the data range.

There are several models that could have been used to fit growth response from the digitized phytoplankton cell concentration and growth rate data (see Figure 3). One of the most common and widely used models for modeling the growth of plants and animals is the Gompertz model (as modified by Zwietering et al., 1990). However, the Gompertz model does not include an explicit parameter to account for the change in growth rate as organisms transition between exponential and stationary phases. Other possible contenders are the Blackman model (Blackman, 1905) and the Bannister model (Bannister, 1979), both of which were initially formulated to describe a photosynthesis versus irradiance curve (Jones et al., 2014). Both of these models are part of a family of modeling equations that describe a rectangular hyperbola-like curve (Jones et al., 2014). The Blackman model, however, defines a bilinear relationship in

which there is a transition from a constant exponential growth rate to no growth without any decrease in rate during an extended transition. The best choice for a modeling equation in this scenario is the Bannister model because it includes a parameter for flexible curvature which better accommodates changes in biomass accumulation due to changes in cell size or fluorescence (see next chapter) in addition to cell division. These can cause a deviation from the Gompertz model.

Figure 3 illustrates the differences in fit of three models in a plot of ln-transformed cell concentrations over time. All models have been modified to include a non-zero intercept. The Blackman and Bannister model have also been modified to include a lag-phase, which is explicit in the Gompertz model. These alterations are important because a zero intercept assumes that there is a starting population of one cell (ln[1]=0), and if the initial value of the population parameter (cell concentration, fluorescence, etc.) is not equal to 1, the intercept value will be non-zero. Including a lag-phase parameter in the equation allows for tracking both an actual lag in growth but can also account for an initial period of observation in which the population parameter is below the lower limit of detection (LLD) of the detector. One of the major limitations of all these models is that they cannot accommodate a decrease in the population parameter after the culture has reached stationary phase. This limitation was not a significant concern for this scenario, since the data that was digitized did not go far enough into stationary phase that a loss of cells was observed. It was an issue when the same model was applied using fluorescence as the population index (Chapters 3 and 4), as in some cases there was a decline in bulk fluorescence in stationary phase, consistent with down-regulation of pigments during nutrient stress (Geider et al., 1998).

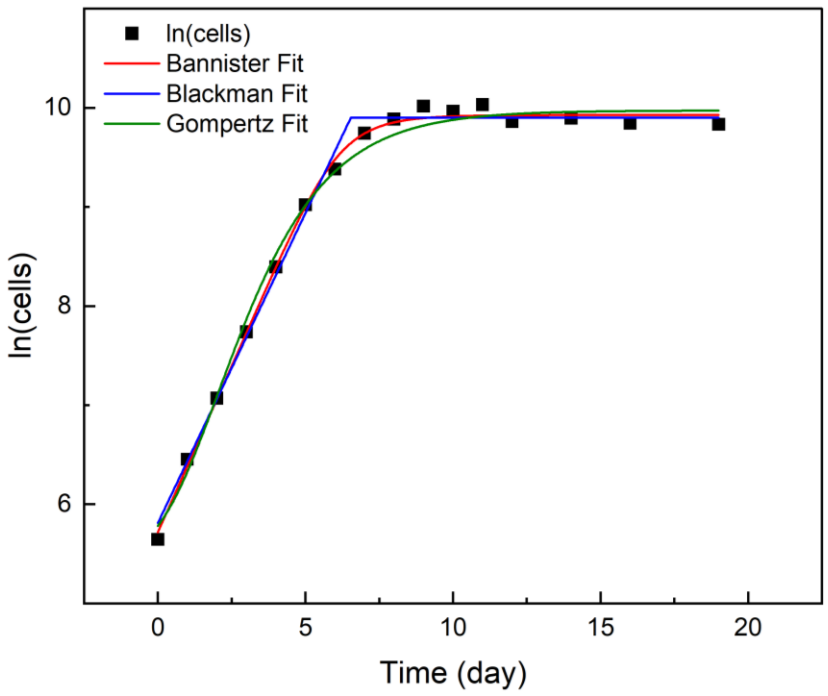

Figure 3: A comparison of model fits for the Bannister (red), Blackman (blue), and Gompertz (green) models, all modified to include non-zero y-intercept. The Blackman does not parameterize the curvature in the data characteristic of the transition between exponential and stationary phase (RMSE = 0.061). Curvature in the Gompertz model is fixed and it underestimated growth during the transition (RMSE = 0.129). The Bannister model has a parameter that allows for different rates of curvature and gave a better fit with the data (RMSE = 0.022).

Digitizing the data yielded either the cell concentrations or growth rates against the time that each data point was collected. For articles that listed cell concentrations, the natural log of the cell counts was calculated and then fit against time using Equation 1, the modified Bannister model (Bannister, 1979),

$$\ln[cells_t] = \left(\ln\left[cells_{fin}\right] - \ln[cells_{init}]\right) \cdot \frac{day}{((t_{stat})^b + t^b)^{\frac{1}{b}}} + \ln[cells_{init}] \quad (1)$$

Where t is time (d) and t_{stat} is the time to stationary phase; $cells_{init}$, $cells_{fin}$,and $cells_t$ are cell concentrations (cells mL^{-1}) at $t = 0$, in stationary phase, and at time t; and b (dimensionless) is a parameter that defines the curvature as the growth rate declines in the transition between exponential and stationary phase.

The maximum and instantaneous growth rates were determined from these fits. The instantaneous growth rates were then normalized to the maximum growth rate to allow comparison between cultures in a dimensionless analysis. The normalized growth rates were then plotted versus their corresponding pH (Figure 4 versus Figure 2) and fit with either a biphasic (Equation 2a & b) or 1st-order kinetic model (Equation 2a & c) that describes the decline in growth rate above a threshold pH value (modified from MacIntyre et al., 2018);

$$\frac{\mu}{\mu_{max}} = 1 \text{ for pH} \leq \text{pH}_{\text{Th}} \quad (2a)$$

and

$$\frac{\mu}{\mu_{max}} = (1-\alpha) \cdot \exp\left(-k_1(pH - pH_{Th})\right) + \alpha \cdot \exp\left(-k_2(pH - pH_{Th})\right)$$

$$\text{for pH} > \text{pH}_{\text{Th}} \quad (2b)$$

or

$$\frac{\mu}{\mu_{max}} = \exp\left(-k \cdot (pH - pH_{Th})\right) \text{ for pH} > \text{pH}_{\text{Th}} \quad (2c)$$

where α (dimensionless) is a coefficient that partitions the biphasic response and varies between 0 and 1, k_1 and k_2 and k (pH^{-1}) are sensitivity coefficients that relate to the slopes, and pH_{Th} is the threshold pH above which growth rates decline with pH. The threshold model of pH change is

utilized here as it is a common model that allows "shouldering" in various studies of inactivation (Hijnen, 2006; Weavers & Wickramanayake, 2001). Although the focus of these studies is UVC photoinactivation rather than pH limitation, the mechanistic underpinning of progressive debilitation often with "tailing" is supported by observations of "shouldering" in the data followed by progressive debilitation in both scenarios.

For the articles that reported growth rates rather than cell concentrations, the fitting with Equation 1 was omitted, and the digitized data was fit only with the biphasic or 1st-order kinetic model (Equation 2). The determination to fit with either the biphasic vs 1st-order model was made based on the values of k_1 and k_2 in the biphasic model. If k_1 and k_2 and k were not significantly different, then the 1st order kinetics model was used, but if k_1 and k_2 were significantly different, then the biphasic model was used.

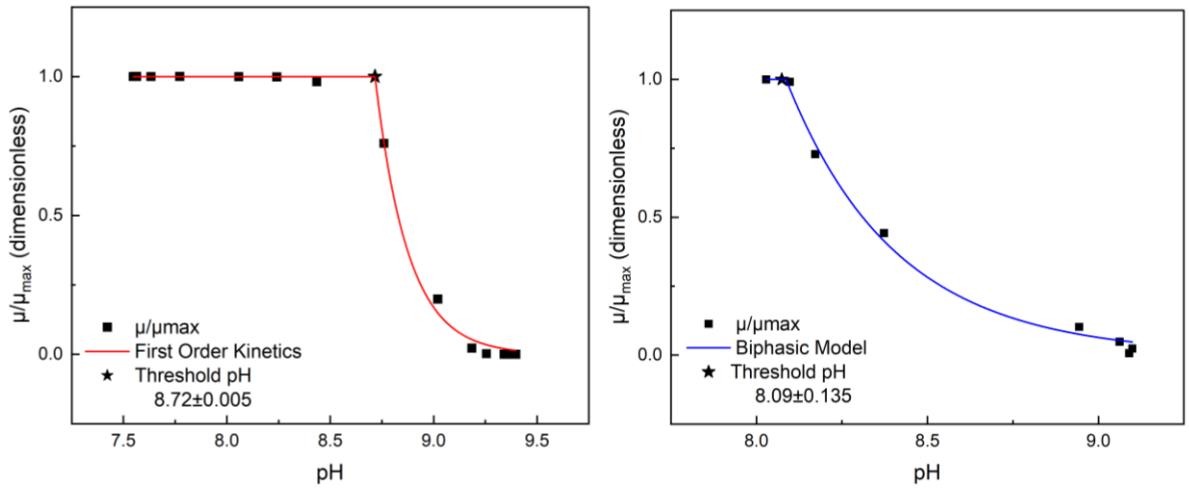

Figure 4: (a) Example of the 1st Order Kinetic model fit for *Heterocapsa triquetra*, NIES 7 (Berge et al., 2012), threshold pH 8.72±0.005. And (b) Example of the Biphasic model fit for *Pseudo-nitzschia granii*, PG (Lundholm et al., 2004), threshold pH 8.09±0.135.

The fits from each model used, either biphasic or 1st-order, were then used to calculate a corresponding normalized growth rate for pH increments of 0.005, from which the pH values at which there was a 10% and 90% reduction in growth were extracted. Dot plots of these pH values and of the threshold pH, were created to compare responses between classes of phytoplankton. Figure 4a shows the model fit using the 1st order kinetics model and Figure 4b shows the model fit using the biphasic model. Data sets that could not be fit with the models because there were fewer data points than fit parameters were omitted. Additionally, the species investigated by Berge et al. (2010) could not be fit with the models because no threshold pH could be determined (the experiments did not raise the pH high enough to cause any notable decrease in growth rates). These are also excluded from consideration. Primer 7 software (PRIMER-e v7.0.21) was used to test for differences between the taxonomic groups in Figures 6, 7, and 8 using the statistical test of analysis of similarity (ANOSIM).

2.3.2 Time-series of pH

Time-series of pH data were obtained from the literature review and from sites in the coastal Atlantic (Figure 5) with long-term and publicly accessible monitoring programs to determine variability in situ. Data are from Mariager Fjord, Denmark (Hansen, 2002), the National Estuarine Research Reserve System (Sapelo Island, GA; Waquoit Bay, MA; Chesapeake Bay, MD; NERRS), the Marine Ecological Time Series (Wadden Sea and Northern Baltic Sea; O'Brien, 2014), and the Bedford Basin Time Series (MEOPAR). The average salinity of the surface waters at the monitoring sites were: 16-17 (Mariager Fjord), 8.5 (Chesapeake Bay), 30 (Waquoit Bay), 28.7 (Sapelo Island), 30 (Wadden Sea), 3.5 (Northern Baltic Sea), and 30 (Bedford Basin). The temperatures of the surface waters at the monitoring sites exhibited a much wider range of between -1 and 33.2°C depending on latitude and season. The majority of

these sites reside in locations where there is lots of anthropogenic input in the form of riverine inputs and farming runoff, allowing for excess nutrients to be present in the surface waters.

The average monthly pH values were determined by averaging one year's data (National Estuarine Research Reserve System and MEOPAR) or by digitizing already averaged monthly data (Marine Ecological Time Series and Hansen, 2002) from surface water samples. Sampling intervals were not listed for data collected from the Marine Ecological Time Series or for Hansen, 2002; however, the sampling interval for the data collected from the National Estuarine Research Reserve System was every 15 minutes and the sampling interval for data collected from MEOPAR was once per week. All the averaged time series data was then collated into a database and combined into a single graph (Figure 1b).

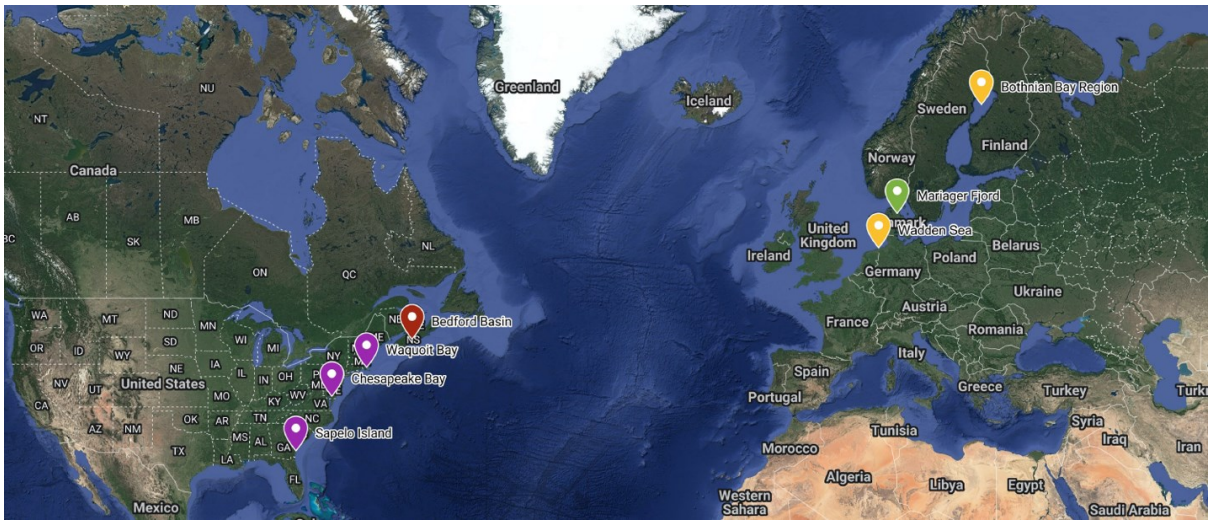

Figure 5: Map of sites where time-series data of pH (Figure 1b) were collected.

2.4 Results

Except for Chesapeake Bay, Bedford Basin, and Mariager Fjord, the time-series records of pH in situ ranges from about 7.7 to 8.3 and are relatively constant throughout the year (Figure

1b). The pH in Chesapeake Bay and Bedford Basin is lower than all other sites at about 6.8 to 7.2, likely due to lower buffering capacity and terrestrial inputs of humic and fulvic acids. The other outlier is Mariager Fjord, where the average pH ranges from 8 to about 8.8 within a year as a result of eutrophication and high summer-time productivity (Hansen, 2002).

The threshold pH where the growth rate begins to decline, pH at which there is a 10% reduction in specific growth rate, and pH at which there is a 90% reduction in specific growth rate are compared for six taxonomic groups of phytoplankton in Figure 6. For all groups, the average threshold for each category is above pH 8.5, as are the 10 and 90% reduction in growth rate. In the context of OAE, this would correspond to addition of c. 330 μmol kg^{-1} of alkalinity in Ketch Harbour, NS (Figure 1c). The ANOSIM comparing all taxa concluded that there is a statistical difference between groups ($p = 0.001$), with the major differences being between dinoflagellates and all other groups, except for prymnesiophytes, and between cryptophytes versus diatoms. The comparisons of statistical differences between taxonomic groups are in Table 1. Running a similarity percentage analysis (SIMPER) concludes that the factor driving this difference is the pH at which μ was reduced by 90% in most cases, but in comparisons with dinoflagellates the difference is more evenly distributed between the three pH factors.

Table 1: R significance level (ANOSIM) for differences between taxonomic groups in Figure 6. Variables include the threshold pH, the pH for a 10% reduction in growth rate, and the pH for a 90% reduction in growth rate. A * indicates a significant result.

	Crytophyte	Prymnesiophyte	Chlorophyte	Raphidophyte	Diatom	Dinoflagellate
Crytophyte						
Prymnesiophyte	0.2					
Chlorophyte	0.2	0.2				
Raphidophyte	1	0.33	0.25			
Diatom	0.0071*	1	0.1	0.14		
Dinoflagellate	0.001*	0.89	0.003*	0.019*	0.054*	

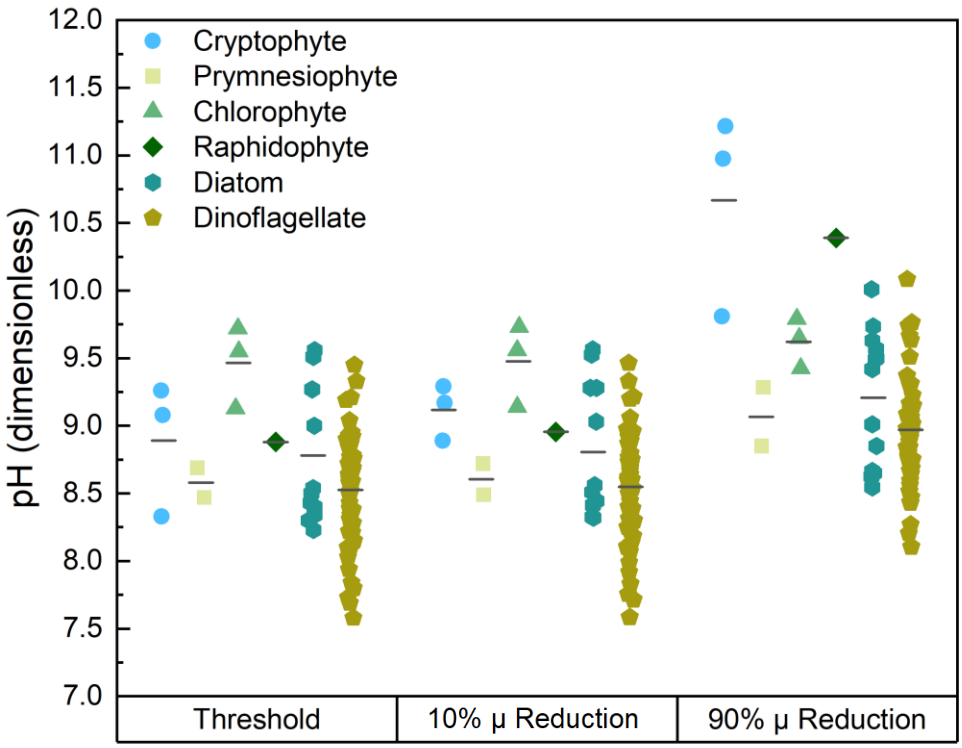

Figure 6: Comparison of the estimate of pH above which there is an impact on growth rates (pH_{Th}), the pH at which there is a 10% reduction in growth rates, and the pH at which there is a 90% reduction in growth rates for a range of taxonomic groups. Each point represents a different species or different growth conditions. The black lines indicate the mean pH values for each group.

There is wide variability in pH sensitivity within taxonomic groups (Figure 6) and while the widest range of threshold pH values and the lowest observed values are found in the dinoflagellates, this may only reflect the large differences in sample sizes between groups. As can be seen in Figure 7, the variability within even a single species can be large, ranging over 1.5 pH units. This is a direct result of the physiology of *H. triquetra* and will be discussed later in this chapter. The average pH value for all three categories are lower in *Heterocapsa triquetra*

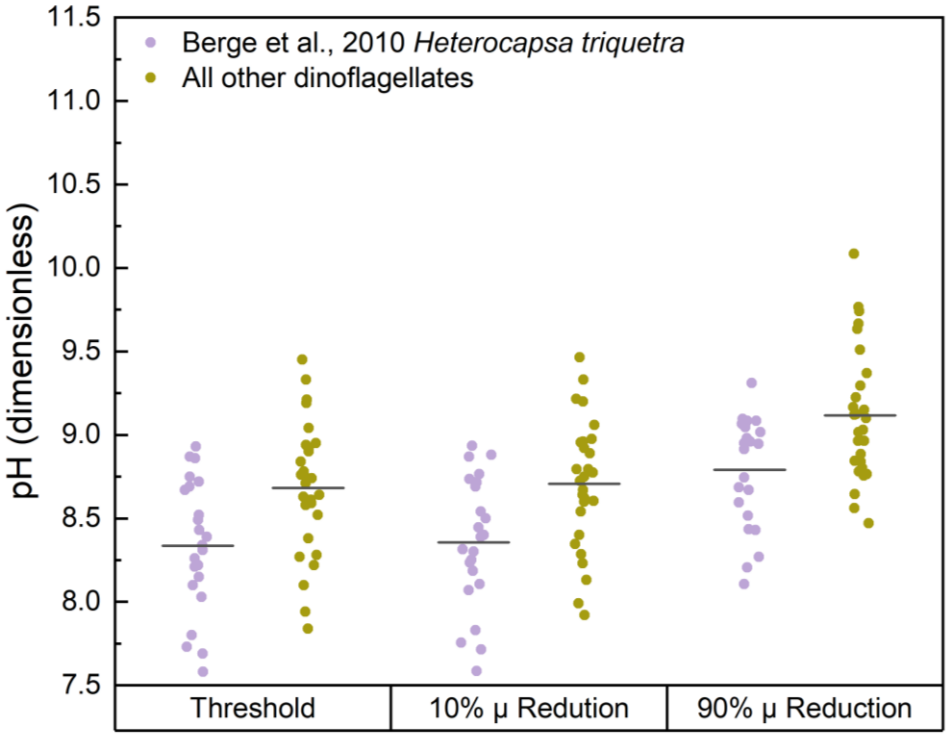

Figure 7: Comparison of the estimate of pH above which there is an impact on growth rates (pH_{Th}), the pH at which there is a 10% reduction in growth rates, and the pH at which there is a 90% reduction in growth rates. The comparison is between 23 strains of *Heterocapsa triquetra* kept under the same conditions and 28 other species of dinoflagellates under a variety of conditions. Each point represents a different species or different growth conditions, and the black lines represent the mean pH values.

than in the other dinoflagellates; however, statistical testing using ANOSIM indicates that the two dinoflagellate groupings are not statistically different from each other.

The last comparison with data collected from the literature is between strains of *Ceratium* that have been maintained at constant pH in semi-continuous culture versus those where the pH

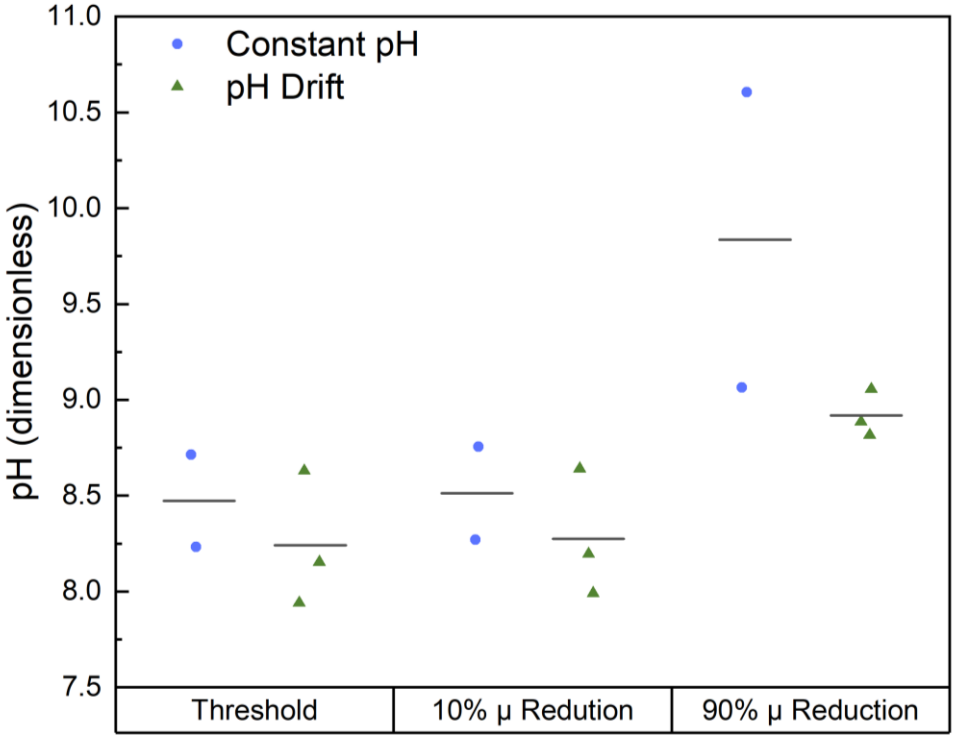

Figure 8: Comparison of the estimate of pH above which there is an impact on growth (pH_{Th}), the pH at which there is a 10% reduction in growth rates, and the pH at which there is a 90% reduction in growth rates between *Ceratium furca*, *C. fusus*, and *C. tripos* that have either been kept at a constant pH or where the pH was allowed to drift. The constant pH curve for *Ceratium tripos* could not be fit with the model because there was no decrease in growth rate with increasing pH, and thus was omitted. Each point represents a different species or different growth conditions, and the black lines represent the mean pH values.

was allowed to drift naturally in batch culture. This comparison can be seen in Figure 8. The average threshold pH in the constant pH experiments is not statistically different than the drift experiments. Note that in the case of *C. tripos*, there was no detectable decrease in growth rate with pH in the semi-continuous cultures, although there was in the batch-drift cultures. As the absence of an effect could not be parameterized within the framework of the model, the semi-continuous culture is not presented in Figure 8. Understanding this comparison is vital for determining how short-term changes in pH differ from long-term acclimation to a stable pH.

2.5 Discussion

The measurement of pH is a powerful tool for assessing the marine environment, indicating both the degree of acidification and alkalization. There is, however, a large degree of natural temporal variability of pH on both small (30 days; Hofmann et al., 2011) and large time-scales (year; Figure 1b). Figure 1b demonstrates that there is also wide geographical variability with average pH values ranging from 7 to 8.25 in coastal areas. The anticipated rise in pH to c. 8.3–8.5 with OAE corresponds to addition of c. 50 μmol L^{-1} hydroxide at the proposed pilot site in Bedford Basin. However, the degree of alkalization possible before reaching this value is highly dependent on the in situ pH before addition. High temporal variability in pH could have negative effects on the degree of functionality of OAE to remove carbon from the atmosphere depending on mixing rates, dissolution, and tidal cycles, and high geographical variability suggests that careful consideration must be made on where the best locations are to release hydroxide for OAE to prevent detrimental effects on phytoplankton populations.

Phytoplankton have metabolic mechanisms in place to assist with changing environmental conditions, whether the conditions are positive or negative. One such adaptation is a difference in the form of Rubisco present in the cell. There are two primary forms of Rubisco enzymes present in cells: Form II, the L_2 structure, is found in peridinin-containing dinoflagellates such as *Heterocapsa triquetra*, *Ceratium spp*., etc., while Form I, the L_8S_8 structure, is found in the other algae and cyanobacteria (Badger et al., 1998). Both forms switch between the carboxylase and oxygenase reactions for the photosynthetic enzyme Rubisco (Raven et al., 2014) but the Form II has a lower affinity for CO_2 than the Form I (Iñiguez et al., 2020). The carboxylase reactions occur when carbon is readily available at the active site of Rubisco, but if carbon availability is low, the oxygenase reaction will occur with oxygen as a substrate instead, because of the similarity in the conformation between the two oxygen atoms in CO_2 and O_2 (Badger et al., 1998). The oxygenase reaction is costly, leads to a net carbon loss from the cell, and confers no benefit to the cell. The majority of phytoplankton favour the caraboxylase reaction by increasing internal CO_2 concentrations through the use of CCMs when CO_2 is not saturating in the surrounding environment (Raven et al., 2017). Function of the CCM is more important to organisms with Form II, which may underlie the differences between the dinoflagellates and the other taxa in the comparison (Figure 6).

The three components of the CCM are active HCO_3^- uptake through a co-transporter, active CO_2 transport, and/or carbonic anhydrase. The configuration of these components varies between different taxa of phytoplankton (Colman et al., 2002), suggesting that there are various combinations in which the CCMs can be oriented depending on the environmental pressures. One of the most common configurations is with all three components on the cell's external membrane and an additional carbonic anhydrase on the chloroplast membrane. When the

external carbonic anhydrase is actively converting HCO_3^- to CO_2, it releases OH^-, which then causes an increase in the pH of the phycosphere, the area surrounding the cell (Nimer et al., 1997). A pH increase in the phycosphere could cause a disruption in the active uptake of HCO_3^- by the OH^- co-transporter, reducing its efficiency. Understanding how these internal processes may be impacted by elevated pH is necessary for a mechanistic understanding of how phytoplankton will respond to OAE, although it is not required for observation and classification of the effects (e.g., Figure 6).

For all taxonomic groups investigated in Figure 6, the mean threshold pH is above 8.5, meaning about 50% of species would not be impacted by the anticipated pH increase associated with OAE. The other 50% of species might be impacted. The large variability within taxonomic groups could be a result of adaptive differences between species and within-species isolates. Another possible reason for observed differences is taxonomic variability in response to covarying factors, such as the concentrations of DIC (Hansen et al., 2007; Søderberg & Hansen, 2007; Søgaard et al., 2011) or light intensity (Søderberg & Hansen, 2007; Nielsen et al., 2007). Unfortunately, these factors can not be assessed directly for the literature as only 3 studies of the 13 reviewed list the DIC availablity, and only 2 included variations in light intensity in the experimental design. The taxonomic group that is the most statistically different from the others is the dinoflagellates. While this might simply be because there is more complete sampling of this group than any of the others due to them being a common study species for the Hansen research group (Hansen, 2002; Hansen et al., 2007; Berge et al., 2010; Berge et al., 2012; Søderberg & Hansen, 2007), it might also reflect fundamental differences in their physiology and ecology. Dinoflagellates are a focus for the Hansen research group because they dominate during the summer when pH is most likely to be high in Mariager Fjord. Their ability to dominate over

other phytoplankton species when their sensitivity to pH suggests they should be the most impacted might be attributed to their frequent use of mixotrophy rather than photosynthesis. Mixotrophy is the combination of phototropy and phagotrophy (Stoecker, 1999), which confers an advantage for nutrient acquisition during stratification events (Margalef, 1978). It might also confer an advantage in coping with elevated pH.

In relation to the extensive range observed for all dinoflagellates, Figure 7 examines a breakdown of the variability within a single species compared to the taxonomic group. Most notably, the average threshold pH of dinoflagellates increases when *H. triquetra* is removed and made into its own category. While the average threshold of *H. triquetra* is lower than the remaining dinoflagellates, it is still higher than 8.3, suggesting that the majority of isolates would not be affected by OAE. The specific strains of *H. triquetra* examined here were all monitored by Berge et al. (2012) in pH drift experiments and classified as either having been cultivated for longer than 10 years or less than 10 years. There was not a trend in pH tolerance based on the length of time since isolation; however, the isolation location, average cell size, and average growth are more likely to influence the tolerance to pH (Berge et al., 2012). Isolation location plays a role since the natural variation in pH can be quite large (Figure 5) and is likely to exert a selective influence on the configuration of CCMs based on DIC availability. Cell size and growth rate are also likely to be significant contributors to the threshold pH since a small cell will have a larger surface area to volume ratio leading to more exposure to the surrounding environment, and a faster growth rate would allow the species to acclimate to higher pHs faster (Berge et al., 2012). Nonetheless, the overall conclusions from Figure 7 suggest that different isolates of a single species can exhibit a wide adaptive range of tolerance to pH.

Quantifying the impacts of pH and other experimental measures is necessary for predicting the effects that OAE can have on the marine environment. Nevertheless, exploring the difference in response when species are or are not allowed to acclimate to the changing pH is equally vital, which is illustrated in Figure 8. The difference in means between 2 of the 3 strains of *Ceratium* kept at a constant pH versus those in which the pH was allowed to drift is not statistically significant. The ability of both cultures to tolerate the elevated pH in a similar manner could be because other stressors (DIC, light, nutrient availability) do not impact successful growth, or that the cells in the pH drift cultures were able to adapt to the rate of change in these stressors. In contrast, the constant pH *C. tripos* did experience a difference in response from the pH drift *C. tripos*, with no observable threshold in the constant pH culture. The difference could be due to the stressors mentioned previously, or because of a difference in acclimation time. However, both of these experimental set-ups are a mismatch for the likely discharge of hydroxide into well-mixed waters where exposure time will be much shorter. Thus, it is not possible to accurately predict the response of phytoplankton to OAE from the data examined.

The data collected in Figures 6, 7, and 8 (chronic exposure) will be utilized to compare the impact of OAE (transient exposure) on representative cultures of near-shore species of phytoplankton. This will be done by comparing the chronic response for the representative species with the taxonomic data from Figures 6, 7, and 8 to confirm that predicted trends in growth rate thresholds are being followed. Viability will also be examined because it is possible for growth rates to remain high due to vital cells contributing to fluorescence (proxy used for growth) even when they are no longer able to reproduce. Physiological impacts will be examined as, in combination with growth rates and viability, it gives context for the range of OAE likely to

be tolerated by phytoplankton. When combined this can give a more holistic view of the impact of OAE on coastal phytoplankton species.

2.6 Conclusion

The data examined above investigates the impact of elevated pH on the growth rates of various taxonomic groups of phytoplankton. Intriguingly there is large variability within taxonomic groups, and even within species, as to what value the mean threshold tolerance for pH falls on. The overarching conclusion is that a combination of pH and DIC availability, and to a lesser extent light attenuation and nutrient availability, are influencing the threshold tolerance, as well as the individual's adaptive characteristics. Overall, there are a number of internal cellular processes (CCMs, Rubisco, enzymatic processes, etc.) that work together in determining a cell's response to elevated pH and changes in DIC availability.

CHAPTER 3

ASSESSMENT OF A LOW-VOLUME VIABILITY ASSAY

3.1 Abstract

A current detection method, the Serial Dilution Culture – Most Probable Number Assay (SDC–MPN), was used in a modified format to assess the impact of Ocean Alkalinity Enhancement (OAE) on phytoplankton viability. The modified assay increases throughput and reduces the human effort needed for monitoring by using polystyrene cell culture plates as opposed to borosilicate glass tubes. However, method validation is needed before experimentation to ensure that the data being collected is robust. Results from the green alga *Tetraselmis suecica* suggested the modified SDC–MPN is a valid method; however, results from the diatom *Thalassiosira pseudonana* were varied, prompting further investigation. Potential hypotheses for inconsistent and low growth of *T. pseudonana* on the plates included leaching of growth inhibitors, the culture volume being too low, or an essential element missing from the medium. Hypothesis testing following the strong inference method of Platt (1964) was conducted to determine the underlying issue of poor growth in *T. pseudonana*. The results determined that the primary factor in the decreased growth of *T. pseudonana* was the absence of selenium from its growth medium, f/2. The medium in which *T. suecica* is grown, L1, contains selenium which explains why results were valid with this species. The addition of selenium to the f/2 medium was then adopted for future experiments using polystyrene cell culture plates.

3.2 Introduction

The Serial Dilution Culture – Most Probable Number Assay (SDC–MPN) has a varied history of use for detecting viability in microbes (MacIntyre et al., 2018). It was first used by McCrady (1915), who diluted the bacterium *Bacillus coli* in an attempt to accurately and precisely determine the number of bacteria present in a tube (*i.e.*, the most probable number of viable cells in the parent sample). Subsequent iterations of the assay came from Allen (1919) and Throndsen (1978) who made alterations to the assay for use with phytoplankton and refined the methods of the assay, respectively. The next development came from MacIntyre et al. (2018) who began using daily measurements of fluorescence to create a time-course instead of cell counts, as had been done previously, and who developed a Quality Control/Quality Assessment (QC/QA) protocol to minimize the risk of false negative results. In this chapter, the assay is multiplexed, using polystyrene cell culture plates as opposed to multiple, independent borosilicate glass tubes. This change increases sample throughput by reducing personnel time by about 30 times.

To validate this change, QC/QA criteria must be met to ensure that best practice protocols are being followed and there is repeatability between experiments. The requirements are as follows.

1. Growth in the polystyrene plates must be observable and repeatable between replicate wells. This requires a sensitive instrument that is capable of measuring fluorescence from small volumes and homogeneity of response between wells.

2. The assay must not underestimate viability. For untreated, control cultures grown in semi-continuous, balanced growth, Relative Viability (RV), defined as the ratio of MPN to the total cell count, should be statistically indistinguishable from 1.

3.3 Methods

3.3.1 Culturing Techniques

The phytoplankton cultures used for the modified SDC–MPN methods testing were the diatom *Thalassiosira pseudonana*, CCMP 1335, and the green alga *Tetraselmis suecica*, CCMP 906, both of which were obtained from the National Center for Marine Algae and Microbiota (NCMA, East Boothbay, ME, USA). The strains were maintained in balanced growth in semi-continuous culture (MacIntyre & Cullen, 2005) in continuous light at c. 190 µmol photons m^2 s^{-1} at a temperature of 18 ±1 °C. The cultures were grown in 40-mL volumes of f/2 (Guillard, 1975) or L1 (Guillard & Hargraves, 1993) seawater medium in 50-mL borosilicate glass tubes with HDPE screw-caps. Cultures were diluted into fresh media in mid-exponential phase in a laminar flow hood to maintain culture sterility. Culture tubes were flamed upon opening and closing to avoid possible contamination. The borosilicate glass tubes were cleaned by soaking in a 10% hydrochloric acid (HCl) solution, then a 5% Micro-90 cleaning solution (Z281506, Sigma Aldrich), and a second 5% HCl solution. Tubes were rinsed copiously with E-Pure water between each step in the cleaning cycle and then sterilized in an autoclave before use.

Culture fluorescence was measured with a Turner 10AU fluorometer (Turner Designs, USA) following a 30-minute dark acclimation period. Variable fluorescence was measured using a FIRe fluorometer (Satlantic, Canada). The Turner 10AU and the FIRe fluorometers were blanked daily with E-Pure water and filtered seawater, and the FIRe was also standardized with a solution of 100 µmol L^{-1} rhodamine *b* in E-Pure water. The corrected fluorescence was

calculated from the Turner 10AU and the estimates of minimum (F_0), maximum (F_m), and variable fluorescence (F_v) were extracted from the single-turnover induction curve of the FIRe fluorometer using Fireworx software (Audrey Ciochetto, née Barnett, http://sourceforge.net/projects/fireworx/).

Daily specific growth rates, μ (d^{-1}) were calculated from the change in fluorescence measured with the 10AU according to Equation 3 (Wood et al., 2005);

$$\mu = \frac{\ln (F_t/F_0)}{\Delta t} \quad (3)$$

where F_t is the fluorescence (Arb) at the end of the time interval, F_0 is the fluorescence at the beginning of the time interval, and Δt (d) is the length of the time interval. Cultures were assumed to be in balanced growth when the coefficient of variation (CV) for daily estimates of μ and the quantum yield of PSII electron transport, F_v/F_m, were <10% over 10 generations (MacIntyre and Cullen, 2005). Experiments were initiated once a culture was in balanced growth.

3.3.2 Modified Serial Dilution Culture – Most Probable Number Methods

The basic principle of the SDC–MPN is to determine cell viability by monitoring growth (McCrady, 1915; Throndsen, 1978). The method estimates the number of viable cells in a culture diluted serially to the point where no viable cells are present, so that dilutions exhibit no growth. The dilutions are monitored using some proxy for growth; e.g., chlorophyll fluorescence for phytoplankton (MacIntyre et al., 2018). The range of cell detection possible depends on the number of replicate tubes, the number of dilution, the interval between each dilution (here, and conventionally 10^{-1}), and the number of cells in the untreated sample; however, the test has a

finite range and samples that are more concentrated have to be diluted to a greater extent to avoid a categorical estimate instead of a quantitative one (MacIntyre et al., 2018). Table 2 shows the equations needed to calculate dilution ranges, the concentration of viable cells, time to complete the SDC–MPN, and scoring in QC/QA framework developed by MacIntyre et al. (2018). The assumptions here are that cells have been randomly distributed between tiers of dilution and replicates and that growth can be reliably detected in the tubes (Cochran, 1950; Haas and Heller, 1988).

Table 2: Summary of important equations for completing the Serial Dilution Culture – Most Probable Number assay (MacIntyre et al., 2018).

	Equation	Eq. #
Dilution range:	10^{X}, 10^{X-1}, 10^{X-2} Where $X = [\log\left(\frac{MPN_{med}}{N_{viable} \cdot V}\right)] - 1$	4
Concentration of viable cells:	$N_{viable} = MPN \cdot V^{-1} \cdot 10^{-(1-X)}$	5
Time to complete MPN:	$t_{end} = (Y \cdot \ln(2) - \ln\left(\frac{10^{X-x} \cdot N_{viable}}{LLD_{cell}}\right)) \cdot \mu_F^{-1}$ Where *Y* is 5 and *x* = *X*, *X-1*, or *X-2* per the dilution series	6
Positive Scores:	$F \geq 8 \cdot \max(LLD_F, F_{start})\ at\ t \leq t_{end}$	7a
Negative Scores:	$F < 8 \cdot \max(LLD_F, F_{start})\ at\ t = t_{end}$	7b

In practice, the SDC–MPN begins with a parent sample of test (treated) or control (untreated) culture. The parent culture is then serially diluted to the point where there should, theoretically, no longer be any viable cells remaining. This is illustrated in Figure 9: if the parent sample has 60 cells, with serial dilutions of 10^{-1}, the next tier of dilution would have about 6 cells

per tube, the next about 0.6 cells per tube, and the last about 0.06 cells per tube, so there should be no growth in the last tier of dilution (Cullen & MacIntyre, 2016). There is however a finite chance that growth will be observed when not expected, with the chances being about 6 tubes out of 100 showing growth. The tubes are then monitored daily for signs of growth using fluorescence as a proxy for biomass. Equation 6 (Table 2) is used to calculate the time to complete the assay, t_{end} (MacIntyre et al., 2018) with a negligible probability of a false negative result (an underestimate of samples showing growth that can arise if the assay is ended too early). The variable Y is a 5-generation buffer for the lowest tier of dilution to confirm that if viable cells are present, they can grow above the lower limit of detection for the detector, LLD_F (MacIntyre et al., 2018). Once t_{end} has been reached, Equations 7a and 7b (Table 2) can be used to assess the growth/no growth score for each sample of the assay, illustrated in Figure 9 (Cullen & MacIntyre, 2016).

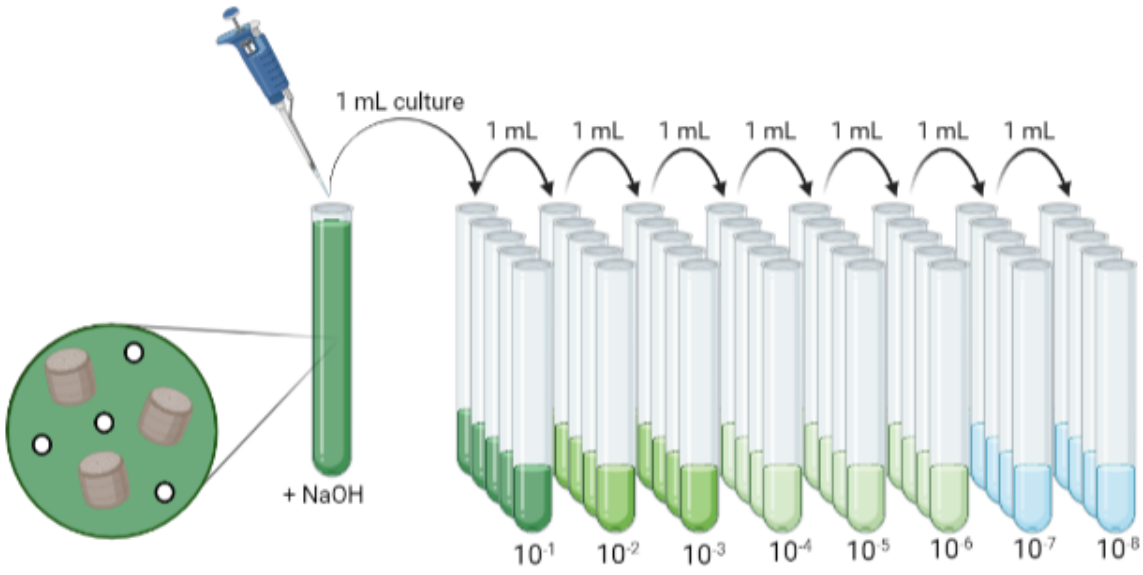

Figure 9: Example of the SDC–MPN.

After all samples have been scored as either positive or negative, an MPN calculator, such as the EPA MPN Calculator (https://mostprobablenumbercalculator.epa.gov/mpnForm), is used to back-calculate the most probable number of viable cells in the original parent sample. This calculation estimates the number of cells in the parent sample from the distribution of growth in the dilutions and the dilution range (Cullen & MacIntyre, 2016). The EPA Calculator also calculates the upper and lower confidence intervals (CI) for the MPN. This is important because the precision of the method is relatively low: the 95% CI is about an order of magnitude around the estimate of the most probable number. So long as the 95% CI of the estimate of RV includes 1 — where RV is the ratio of the estimated concentration of viable cells to the total concentration of cells — then it can be concluded all cells in the sample are viable. This is the expectation for a control culture maintained in balanced growth.

The SDC–MPN assay conducted in individual borosilicate glass tubes described above (Figure 9) has been modified to increase throughput by using sterile polystyrene cell culture plates (Sigma Aldrich). Figure 10 shows an example layout of a 24-well, polystyrene cell culture plate used for an SDC–MPN assay. The serial dilutions for the plates were completed in 10-mL volumes in sterile borosilicate glass tubes. Each plate well was inoculated with 1 mL of volume when 24-well plates were used and 0.5 mL when 48-well plates were used. These volumes were

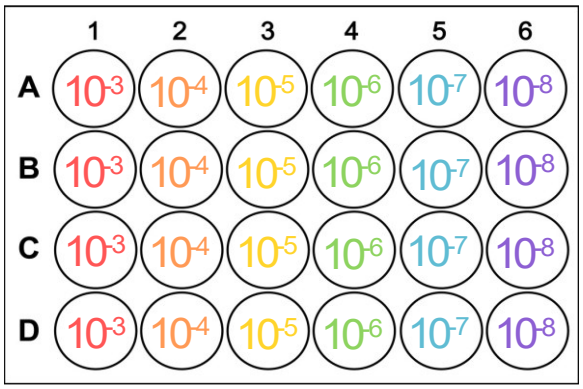

Figure 10: Plate layout showing dilutions in a 24-well polystyrene plate.

based on recommendations from the manufacturer, as well as experiments conducted by other researchers using small volumes of cultures in polystyrene plates (Albrecht et al., 2022; Bannon & Campbell, 2017; Castaldello et al., 2021). All serial dilutions and plate inoculations were completed in a laminar flow hood to maintain culture sterility, and the borosilicate tubes were flamed to avoid possible contamination. The remaining principles of the method remain the same, with fluorescence being used as a proxy for biomass and Equation 6 (Table 2) being used to calculate the assay completion (MacIntyre et al., 2018). Equations 7a and 7b (Table 2) are still used to score each well as either positive or negative for the growth assessment, and the EPA MPN Calculator is then used to back-calculate the most probable number of viable cells in the original parent culture. This is converted to a concentration and expressed relative to the total cell concentration pre-treatment to get the RV of the culture.

3.3.3 Modified SDC–MPN Rationale

The modification to the SDC–MPN is significant as the traditional method is a time-consuming process to collect daily monitoring data (MacIntyre et al., 2018). As shown in Figure 9, there are generally at least three tiers of dilution with five replicates per tier for each treatment. This means that for each treatment, there would be a minimum of 15 tubes to monitor, and this number increases with the addition of a dilutions, replicates, or treatments. Generally, six treatments with six dilutions per treatment are monitored simultaneously with the modified method since each plate can be read in a couple of minutes. However, to monitor six treatments with the regular SDC–MPN , 90 tubes would need to be monitored daily, and each tube takes approximately a minute to read. Monitoring the SDC–MPN using a polystyrene cell culture plate takes approximately 30 seconds, thus reducing the time needed to collect results by about 30

times. The possible drawbacks, such as light availability due to self-shading and possible nutrient limitation, were addressed through the experimental design by dilutions preventing self-shading and excess carbon preventing nutrient limitation.

3.4 Results & Discussion

To conduct the validation of the modified SDC–MPN a set of preliminary tests were completed to ensure that the control cultures met the criterion of RV = 1 (*i.e.*, that the 95% CI includes 1). Tests were conducted with untreated, control cultures of *T. suecica* and *T. pseudonana* using the methods described in Section 3.3.2. An SDC–MPN using *T. pseudonana* was also completed in borosilicate glass tubes to compare the polystyrene plate results with the original fluorescence version of the SDC–MPN. The results of these preliminary tests are show in Figure 11.

The results of the preliminary test SDC–MPN assay completed in borosilicate glass tubes using a control culture of *T. pseudonana* returned the expected value of RV of 1. The same results were not observed with a control culture of *T. pseudonana* grown in the polystyrene cell culture plate, with a 97.55% loss in RV when compared to the borosilicate tubes. However, the control culture of *T. suecica* grown in the polystyrene cell culture plate did retain full viability. The difference in response between the two species indicates as underlying problem when a diatom is grown in polystyrene cell culture plates that must be addressed before further experimentation can occur.

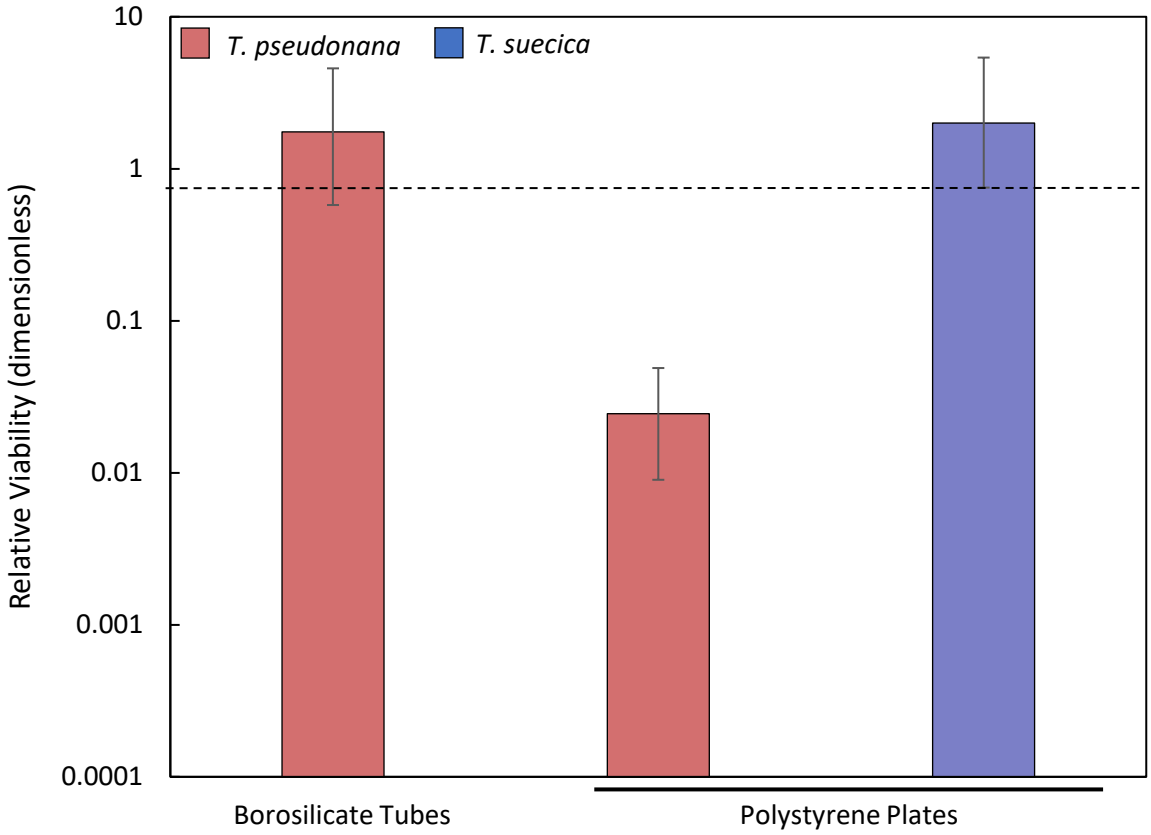

Figure 11: Comparison of Relative Viability (RV) using the SDC–MPN assay of *T. pseudonana* in borosilicate glass tubes, an untreated control culture of *T. pseudonana* in a polystyrene plate, and an untreated control culture of *T. suecica*. Both borosilicate glass tube replicates of control culture *T. pseudonana* and the control culture of *T. suecica* in the polystyrene plate exhibit the expected RV of 1. The control culture of *T. pseudonana* in the polystyrene plate experienced an unexpected 97.55% decrease in RV.

The Strong Inference method proposed by Platt (1964) was used to conduct hypothesis testing on potential causes of the anomalously low viability in *T. pseudonana* grown in polystyrene plates. The steps of the strong inference method are: (1) developing several hypotheses to tackle the research question; (2) designing experiment(s) to rule out one or more

hypotheses at a time; and (3) conducting the experiment(s) to determine a result (Platt, 1964). The series of hypotheses tested for this method were as follows.

H_0[1]: Rigorous cleaning of the plates restores RV.

H_1[1]: Rigorous cleaning of the plates does not restore RV.

H_0[2]: Use of 24-well polystyrene plate instead of 48-well plates restores RV.

H_1[2]: The type of the polystyrene plate does not restore RV.

H_0[3]: The compositions of the growth media has an effect on RV.

H_1[3]: The compositions of the growth media has no effect on RV.

The first hypothesis was prompted by the possibility that plasticizers leaching from the well plates inhibited growth. It was tested by using plates that had been cleaned following a stringent protocol. The cleaning method consisted of 72 hours in a 5% Micro-90 cleaning solution (Z281506, Sigma Aldrich) with an E-Pure water rinse every 24 hours, 12 hours in a 10% HCl solution, a rinse with E-Pure water, and finally 1 hour under an ultraviolet lamp to sterilize the plate. The second hypothesis was tested by conducting the SDC–MPN simultaneously in a 24-well and 48-well polystyrene cell culture plates. The surface area:volume ratio in a single well of a 48-well plate is 0.59 cm^2 mL^{-1} (3548, Corning Incorporated), while in a 24-well plate, the surface area:volume ratio is 0.56 cm^2 mL^{-1} (3527, Corning Incorporated). The surface area:volume ratio for both plates are almost identical; however, because a 24-well polystyrene plate was used to collect the data for *T. suecica* and a 48-well polystyrene plate was used for *T. pseudonana* the two well sizes were compared to determine if this was causing the discrepancy in results. The final hypothesis was prompted by the observation that normal growth

was observed with *T. suecica*, which was grown in L1 medium (Guillard & Hargraves, 1993), but not with *T. pseudonana*, which was grown in f/2 medium (Guillard, 1975). It was tested by comparing the nutrients available in the two different media (L1 and f/2) and determining that selenium was present in L1 but not in f/2. This is of note since selenium is considered an essential trace element for cell growth and is vital for several metabolic functions, including spindle fiber formation during mitosis (Zeng, 2009). Selenium is also generally found in glassware but is almost never found in plasticware. The results from testing these hypotheses are in Figure 12.

The results in Figure 12 show that viability was still reduced in the rigorously cleaned plates, both from the demonstration that the upper 95% CI was <1 and by Analysis of Variance on the replicated treatments vs RV in the borosilicate tubes ($p = 0.025$), so H_0 [1] was rejected. The results in Figure 12 also show that viability was still reduced in the 24-well plate without Se and there was no difference between the 24-well and 48-well plates without Se (overlapping 95% CIs and 95% CI <1) so H_0 [2] was rejected.

The results of the third test (Figure 12) suggest that selenium was likely the main issue when attempting to complete the SDC–MPN in polystyrene plates, although there was a difference between 24-well and 48-well plates. Addition of Se to the medium restored full viability in the 24-well plate (95% CI >1), although it did not in the 48-well plate (95% CI <1). A test of viability in the Se-amended medium in plates vs unamended medium in borosilicate glass tubes was not significant ($p = 0.59$), so H_0 [3] could not be rejected and it was determined that the absence of selenium from the f/2 medium was the underlying issue.

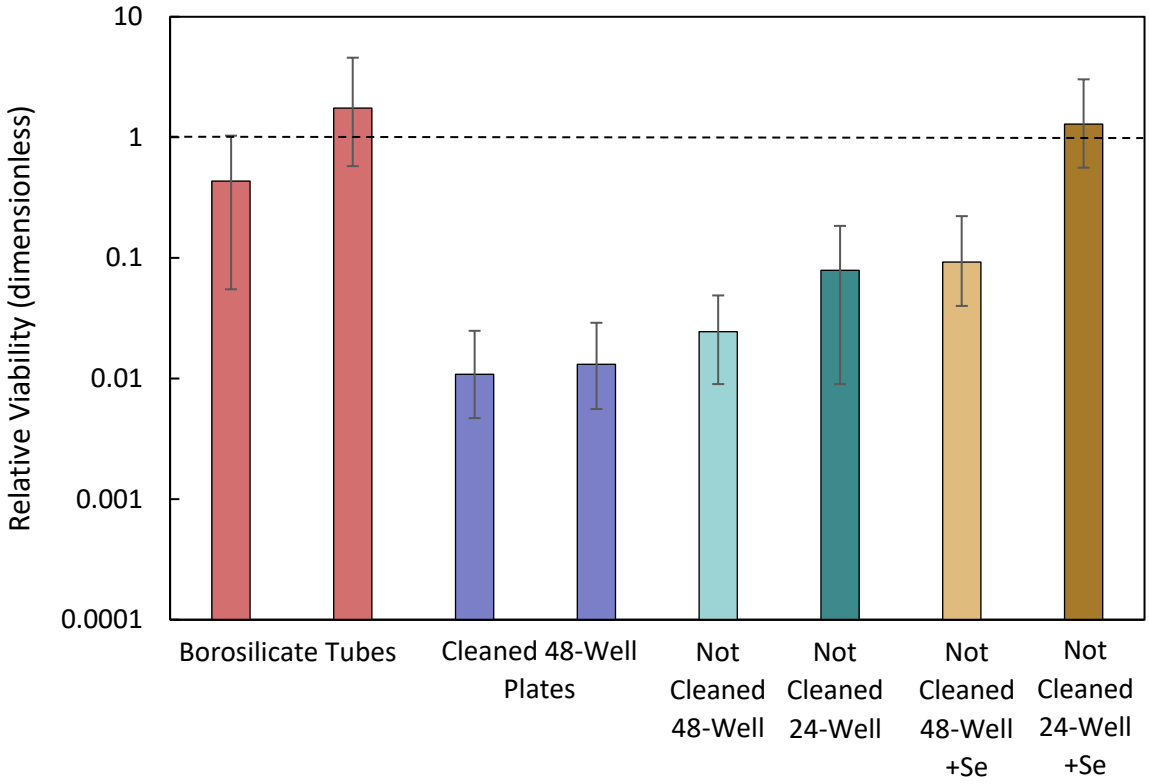

Figure 12: Comparison of Relative Viability (RV) using *T. pseudonana* for testing of the three hypotheses regarding rigorous cleaning of the plates, the type of polystyrene plate, and the composition of the media, respectively, as causative of reduced viability. The RV for the cleaned plates and different plate types are still below 1, except for the 24-well plate with selenium added to the growth medium. Error bars represent the 95% confidence interval.

Achievement of full viability for *T. pseudonana* in Se-enriched f/2 constitutes a validation of the method. The most notable study concerning the requirement of selenium was conducted by Price et al. (1987), in which the growth of *T. pseudonana* was examined in the absence and presence of selenium. They found that selenium was an essential element required for growth. The reason that selenium is an important addition when cultures are grown in

plasticware rather than borosilicate glass is because selenium is not present in plastics, but it is found in glass (Zeng, 2009). Selenium is used for both colouring and decolouring in glass making, depending on the oxidation state of the materials (Scalet et al., 2006). This is why, even without selenium in the media, the cultures were able to successfully grow in glassware, since they could leach the needed concentration from the glass itself.

3.5 Conclusions

Following the strong inference method by Platt (1964), the modified SDC–MPN assay has been proven to be a valid method. Based on the outcome, it is recommended that selenium be added to all growth media, whether included in the recipe or not, to prevent artificial reductions in relative viability not caused by the intended treatment. Moving forward, testing with the modified SDC–MPN can be conducted, and results can be considered robust.

CHAPTER 4

ANALYZING PHYTOPLANKTON RESPONSES AFTER TRANSIENT AND CHRONIC EXPOSURE TO OCEAN ALKALINITY ENHANCEMENT

4.1 Abstract

Ocean Alkalinity Enhancement will almost entirely occur in coastal marine systems, since the *London Convention* prevents human-made matter being released into the open ocean. There is, however, still risk associated with anthropogenically altering the buffering capacity of coastal systems, namely potential negative effects on the organisms that reside there. Thus, the first point of interest in examining OAE, is determining how pH and alkalinity will change with increasing additions of hydroxide, and then secondly determining at what point there will there be an impact on coastal species of phytoplankton. Utilizing previously published data about the impacts of pH on phytoplankton, the modified SDC–MPN, and multiple fluorescence measurements, the effect of chronic and transient exposure to elevated pH and alkalinity on *Thalassiosira pseudonana* and *Pavlova lutheri* was determined. Data from both species suggests that there is a negative impact on growth rates with chronic exposure, but no adverse impacts on species viability or growth rates with transient exposure. Additionally, the photosystem II competence of *T. pseudonana* displays a delay in acclimation to elevated pH and alkalinity which is not present in *P. lutheri*. These results suggest that available literature on phytoplankton responses to elevated pH overestimate the potential impact of OAE if dilution of hydroxide occurs on a transient time scale.

4.2 Introduction

The implementation of Ocean Alkalinity Enhancement (OAE) will need to be land-based, as the release of human-made matter into the open ocean is prohibited under the *Convention on the Prevention of Marine Pollution by Dumping of Wastes and Other Matter,1972*, better known as the London Convention. This means any addition of alkalinity will need to happen along the coast, likely at a previously established outflow or waste pipe, to remain in compliance with the Convention. However, before this can occur, laboratory experiments are required to ensure there are no negative impacts on marine biota, especially phytoplankton as they are the base of the majority of marine food webs and play a significant role in biogeochemical cycling in the ocean (Winder & Sommer, 2012). Specifically, phytoplankton species representative of coastal environments should be tested, as they are the most likely to experience the negative effects of elevated pH associated with the release of OAE.

When determining which species would be the best candidates for examining the impact of OAE, the composition of coastal bloom cycles was examined. Spring blooms are generally composed of phytoplankton with fucoxanthin pigments, which are found in diatoms and prymnesiophytes (Li & Dickie, 2001), and early fall blooms are primarily dominated by diatoms (Li & Harrison, 2008). Thus, it was determined that the diatom *Thalassiosira pseudonana,* and the prymnesiophyte *Pavlova lutheri* would provide good representatives of coastal assemblages. Using the validated modified SDC–MPN (Chapter 3), *T. pseudonana* and *P. lutheri* were tested for reductions in relative viability, photosynthetic competence (as the proportion of functional photosystem II (PSII) reaction centers), and growth rate (μ), following both transient (10-minute) and chronic (days) exposures to hydroxide.

4.3 Methods

4.3.1 Dose-Response Curves for OAE (Transient Exposure)

Cultures of *Thalassiosira pseudonana*, CCMP 1335, and *Pavlova lutheri*, CCMP 1325, (NCMA, East Boothbay, ME, USA) maintained in balanced growth (see Section 3.3.1) were used to create dose-response curves to OAE. These two cultures were chosen as they are characteristic of near-shore, temperate waters, and are characteristic of taxonomies that dominate during the spring and fall blooms. Viability was assessed with the modified SDC–MPN assay following 10-minute exposure to elevated alkalinity and pH. The Quality Control/Quality Assessment (QC/QA) protocols, scoring, and estimates of relative viability are described in Section 3.3.2.

Forty-mL volumes of cultures in balanced growth were alkalized with increasing volumes of a 0.5 M NaOH stock solution in acid-washed and autoclaved 50-mL borosilicate glass tubes to increase the concentration of total alkalinity between 0–1084 μmol kg^{-1} in c. 100 μmol kg^{-1} increments. Table 3 displays the volume of NaOH added, the corresponding pH and total alkalinity, and the concentrations of DIC species for each treatment. Final pH values were between 7.96 and 9.09. The culture and NaOH additions were mixed and allowed to react for 10 minutes before beginning the serial dilution. Subsamples for Turner 10AU fluorescence, FIRe fluorescence, Chlorophyll *a*, and cell counts were collected following the 10-minute incubation. The first dilution in the series (10^{-1}) contained a 1-mL aliquot of the prior tier of treated culture and 9 mL of growth media. The dilution was repeated to give dilutions of 10^{-3} to 10^{-8} in 10x tiers.

Table 3: Carbon system calculations for the different volumes of NaOH. Calculations completed using CO_2SYS software (version 01.05).

NaOH Volume (µL)	pH	Total Alkalinity (mmol kg^{-1})	Total CO_2 (mmol kg^{-1})	HCO_3^- (mmol kg^{-1})	CO_3^{2-} (mmol kg^{-1})	CO_2 (mmol kg^{-1})
0	7.96	2168.3	2000.0	1855.11	127.90	16.99
8	8.18	2281.4	2000.0	1785.82	204.33	9.86
16	8.34	2390.9	2000.0	1710.57	282.90	6.53
24	8.47	2499.9	2000.0	1631.42	363.96	4.62
32	8.6	2628.0	2000.0	1534.87	461.91	3.22
40	8.69	2727.6	2000.0	1457.78	539.73	2.49
48	8.83	2898.7	2000.0	1322.48	675.89	1.63
56	8.87	2950.6	2000.0	1280.81	717.75	1.44
64	9	3126.4	2000.0	1138.45	860.60	0.95
72	9.06	3209.9	2000.0	1070.29	928.94	0.78
80	9.09	3252.0	2000.0	1035.90	963.40	0.70

One-mL aliquots from the dilutions were added to the wells of 24-well polystyrene cell culture plates, with 8 replicates per dilution. Once all the wells had been inoculated, a polypropylene heat-resistant film (TI271G, VWR) was placed over the top to prevent contamination. Plates were placed into glass sandwich boxes also containing small plastic containers with ~100 mL of 1 mmol L^{-1} sodium bicarbonate ($NaHCO_3$). Every day, 400 µL of 10% hydrochloric acid (HCl) was added to the $NaHCO_3$ to create carbon dioxide (CO_2) minimizing the likelihood of the cultures from becoming carbon limited and enriching the headspace of the container with CO_2. This avoids skewing the MPN results due to decreased growth not caused by the change in alkalinity and pH.

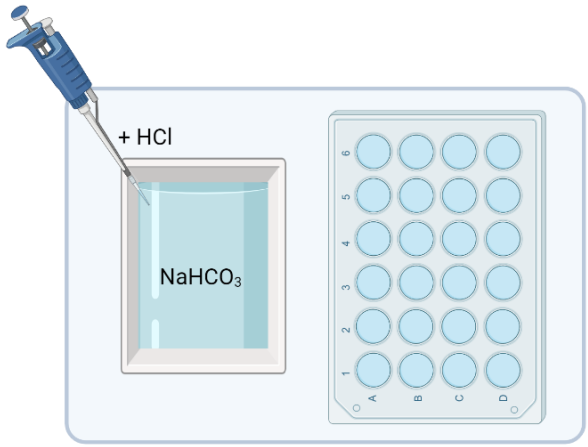

Figure 13: Example of the plate setup in glass sandwich boxes with an additional small container of sodium bicarbonate to reduce carbon dioxide limitation.

The well plates were maintained in continuous light at c. 190 µmol photons m^2 s^{-1} at a temperature of 18 ±1 °C. Daily monitoring was completed by measuring fluorescence with a BioTek Synergy 4 Hybrid Multi-Mode Microplate Reader (Model S4MLFTAD), following a 30-minute dark acclimation period. The software Gen5 (version 1.11.5) was used to collect the output data from the plate reader. Fluorescence values for each well in the plate were determined at multiple sensitivities to ensure accurate readings. Where a well's fluorescence was counted as "overflow", *i.e.*, high enough to saturate the detector, a reading from the next-highest sensitivity was used for the estimate.

Output data was uploaded to a tracking sheet daily, where fluorescence was corrected for both quenching and the sensitivity setting of the plate reader. These corrections resulted in a normalized fluorescence value that can then be used to compare the data from all sensitivities, dilutions, and treatments. The natural log (ln) of the normalized fluorescence for each well was graphed versus day, and the fits from the Blackman bilinear model (Blackman, 1905) modified to include a non-zero intercept (Equation 7) were used to calculate t_{end}, the number of days

needed to monitor growth without risk of a false negative (*i.e.*, a lack of detected growth because the experiment was terminated too early), using Equation 6 in Table 2.

$$ln\big(F(t)\big) = \big(ln\big(F_{fin}\big) - ln(F_{init})\big)\frac{(t-t_{lag})+t_{stat}-|(t-t_{lag})-t_{stat}|}{2\cdot t_{exp}} - ln(F_{init}) \quad (7)$$

where t is time (d); F_{init}, F_{fin}, and $ln(F(t))$ are fluorescence (Arb.) at $t = 0$, in stationary phase, and at time t; t_{lag} is the durations of the lag phase of growth (d); and t_{stat} is the duration of time needed to reach the stationary phase of growth. The Blackman model was used for this calculation because the resolution of data from late exponential into stationary phase was so low, that there was no need for the curvature parameter of the Bannister model.

Following scoring of the growth assays and determination of the concentration of the Most Probable Number of viable cells, Relative Viability (RV) was determined as the ratio of MPN to the concentration of cells in the parent (i.e., treated) culture. Cell concentrations were estimated using a hemocytometer with an inverted microscope (Leica Microsystems). A total of three replicate counts were conducted, and the average count used for the calculation of RV.

4.3.2 Indices of Physiological Status

From each treated culture, 6-mL aliquots were added to a 10-mL borosilicate glass tube. The tubes were aliquoted in a laminar flow hood and flamed upon opening and closing to maintain sterility. Culture fluorescence was then measured using a FIRe fluorometer (Satlantic, Canada) following a 30-minute dark acclimation period. The FIRe fluorometer was blanked with filtered seawater and standardized against a solution of rhodamine *b* in E-Pure water on every use. The estimates of minimum (F_0), maximum (F_m), and variable fluorescence (F_v) were extracted from the single turnover flash (Figure 14) using Fireworx software (Audrey Barnett,

http://sourceforge.net/projects/fireworx/). From these estimates, the maximum quantum yield of photochemistry in PSII (F_v/F_m) can be calculated, which is an indicator of the culture's physiological status. In order to analyze the data, F_v/F_m was plotted versus pH to visually identify any possible trends with increasing treatments and a sensitivity analysis was conducted using a linear regression model to determine where there were statistical differences in F_v/F_m versus pH in each species.

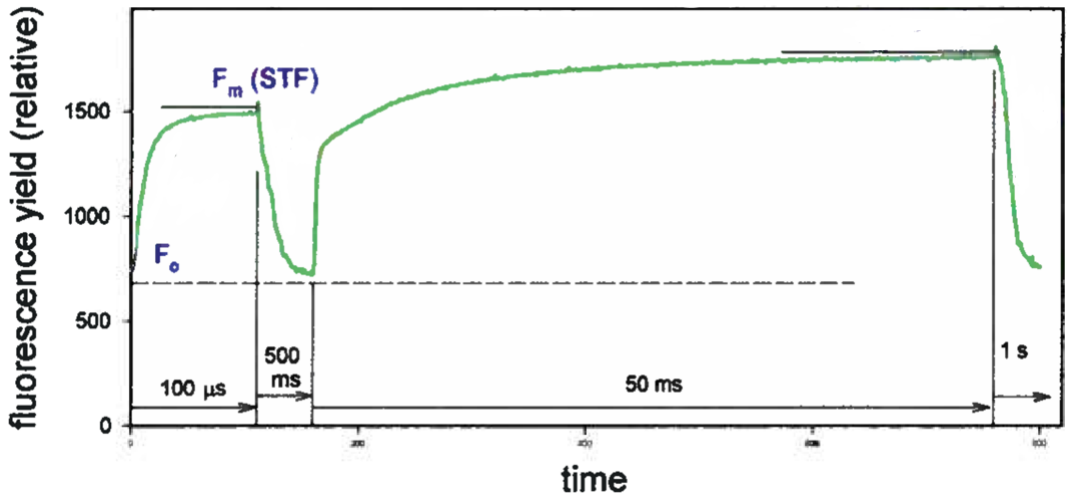

Figure 14: Example of a Fluorescence Induction and Relaxation curve with F_0 and F_m labeled. F_v is calculated from the difference of F_m and F_0 (The Satlantic Fluorescence Induction and Relaxation manual). Results are based on fits to the initial, single-turnover (STF), curve (0-100 µs).

The monitoring of the polystyrene cell culture plate fluorescence described in Section 4.3.1 was also used to help determine the growth rates of the cultures in the SDC-MPN assay. The natural log of the normalized fluorescence value was calculated from the measured fluorescence after being corrected for quenching and sensitivity. The natural log of fluorescence was then graphed versus day and fit with Bannister's model (Bannister, 1979; Equation 1, 2)

modified to include a lag phase to calculate μ_m in Equation 9. This accounts for the inability to detect growth when the fluorescence was below the plate reader's limit of detection. Equations 8a and b show the modified Bannister equation,

$$\ln[F_t] = \ln[F_{init}] \text{ for } t \leq t_{lag} \tag{8a}$$

$$\ln[F_t] = \left(\ln[F_{fin}] - \ln[F_{init}]\right) \cdot \frac{t - t_{lag}}{((t_{exp})^b + (t - t_{lag})^b)^{\frac{1}{b}}} + \ln[F_{init}] \text{ for } t > t_{lag} \tag{8b}$$

where t is time (d); F_{init}, F_{fin}, and F_t are fluorescence (Arb.) at $t = 0$, in stationary phase, and at time t; t_{lag} and t_{exp} are the durations of the lag and exponential phases of growth (d); and b (dimensionless) is a parameter that defines the curvature as the growth rate declines in the transition between exponential and stationary phase.

The maximum (*i.e.*, exponential) growth rate, μ_m (d^{-1}), is then:

$$\mu_m = \frac{\ln[F_{fin}] - \ln[F_{init}]}{t_{exp}} \tag{9}$$

4.3.3 Testing the Impact of Chronic Exposure

Experiments were conducted to test for chronic impacts on *T. pseudonana* and *P. lutheri* in addition to the above tests for impacts from transient exposure to OAE. Cultures were maintained in balanced, nutrient-replete growth as described in 3.3.1. Once in balanced growth, the culture was transferred into a beaker of fresh media in a dark laminar flow hood to maintain culture sterility and treated with NaOH to increase the pH and alkalinity. Treatments consisted of initial pH values of 8.02, 8.13, 8.34, 8.57, 8.69, and 8.82. The treated cultures were divided into two aliquots, one for measurement of pH and one for measurement of growth response. The

latter were transferred into 6-mL sterile, borosilicate glass tubes in replicate, kept in the dark, and immediately read on both fluorometers. The culture tubes were grown into stationary phase, and the in vivo fluorescence was measured every day during this period to calculate the instantaneous growth rates and F_v/F_m.

The daily fluorescence data from the 10AU fluorometer was fit with Equation 8a and b to calculate F_{fin}, F_{init}, and t_{exp}. Equation 9 was then used to calculate the maximum growth rate for each treatment. These were plotted against pH and fit with the 1st-order kinetic model (Equation 2a & c) to determine if there was a threshold value of pH, above which μ_m declined. The mid-exponential values for F_v/F_m, which were selected from the time-point closest to the midpoint between F_{init} and F_{fin}, were plotted against time to test for differences between treatments during the active growth period. This allowed for the data to represent a period of extended exposure to elevated pH without the secondary effects of nutrient stress present during stationary phase.

4.4 Results

4.4.1 Rate of Change in pH

The additions of sodium hydroxide, and thus alkalinity, result in a nonlinear relationship with pH in stirred beakers maintained at 18±1 °C (Section 2.2), which is best explained by a second-order polynomial with an R^2 value of 0.995 (Figure 1c). Figure 15 shows how pH varied with time after alkalization. The rate of change over 4.5 h between T_0 and T_{final} ranges from no significant change ($p = 0.46$) in the smallest alkalinity addition to decreases of 0.013 ± 0.005 to 0.025 ± 0.004 pH units h^{-1} in the rest of the treatments. This means over an exposure period of 10 minutes, as in the transient tests, there would be no detectable change in pH.

The transient exposures were achieved by diluting the treated samples with fresh growth medium. At a dilution of 10^{-2} to 10^{-3}, the pH has returned to the background value, and the effect of the NaOH addition is no longer evident in the pH measurement. This is evident by Figure 16 which displays the reduction in pH with increasing levels of dilution.

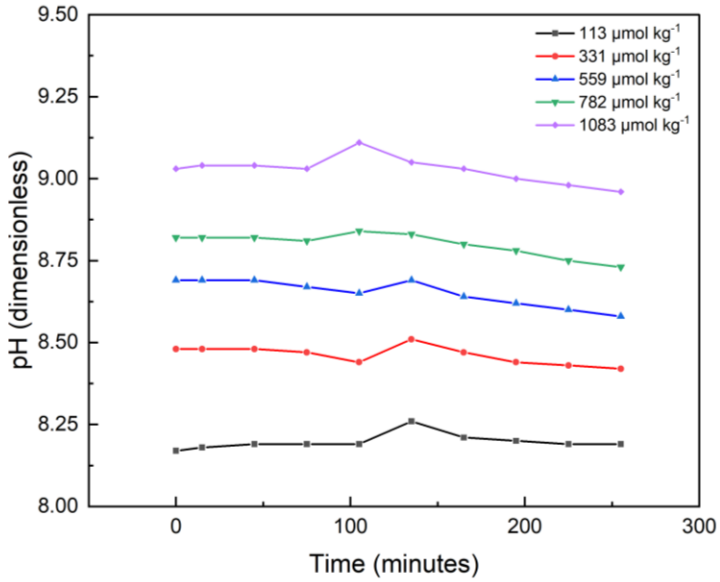

Figure 15: Time course relationship between changes in pH after alkalinity addition.

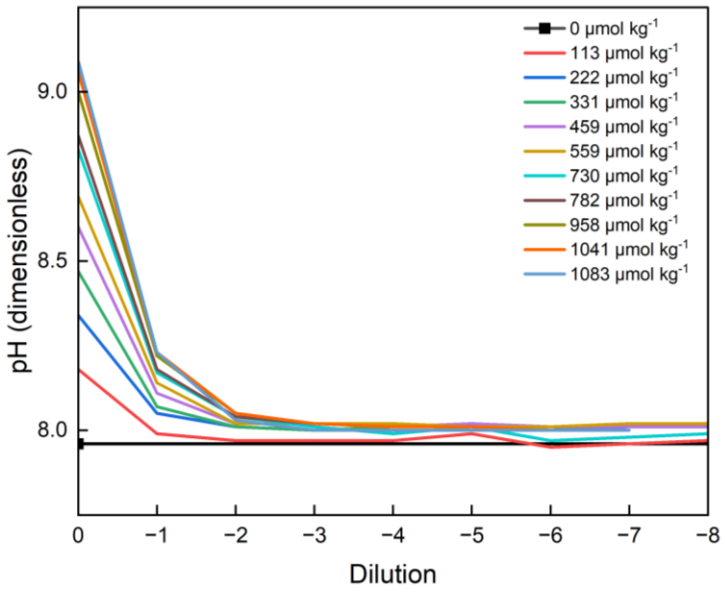

Figure 16: Relationship between pH with increasing 10-fold dilutions for each addition of alkalinity used in the viability assay. The x-axis, dilution, is the coefficient 10^X, where X is 0 to -8.

4.4.2 Transient Impacts

The dose-response curves in Figures 17a and 17b illustrate the lack of impact that the transient exposure to elevated pH had on viability in *T. pseudonana* and *P. lutheri*. Dilutions ranged from 10^{-2} to 10^{-8} depending on the cell counts for the original culture and the concentration of NaOH. In both cases, Relative Viability of 1 was within the 95% Confidence Intervals and Type 1 regressions of Relative Viability on pH were not significant ($p > 0.05$), indicating that there was no impact of transient exposure to increased pH within the range of pH 8 to 9.

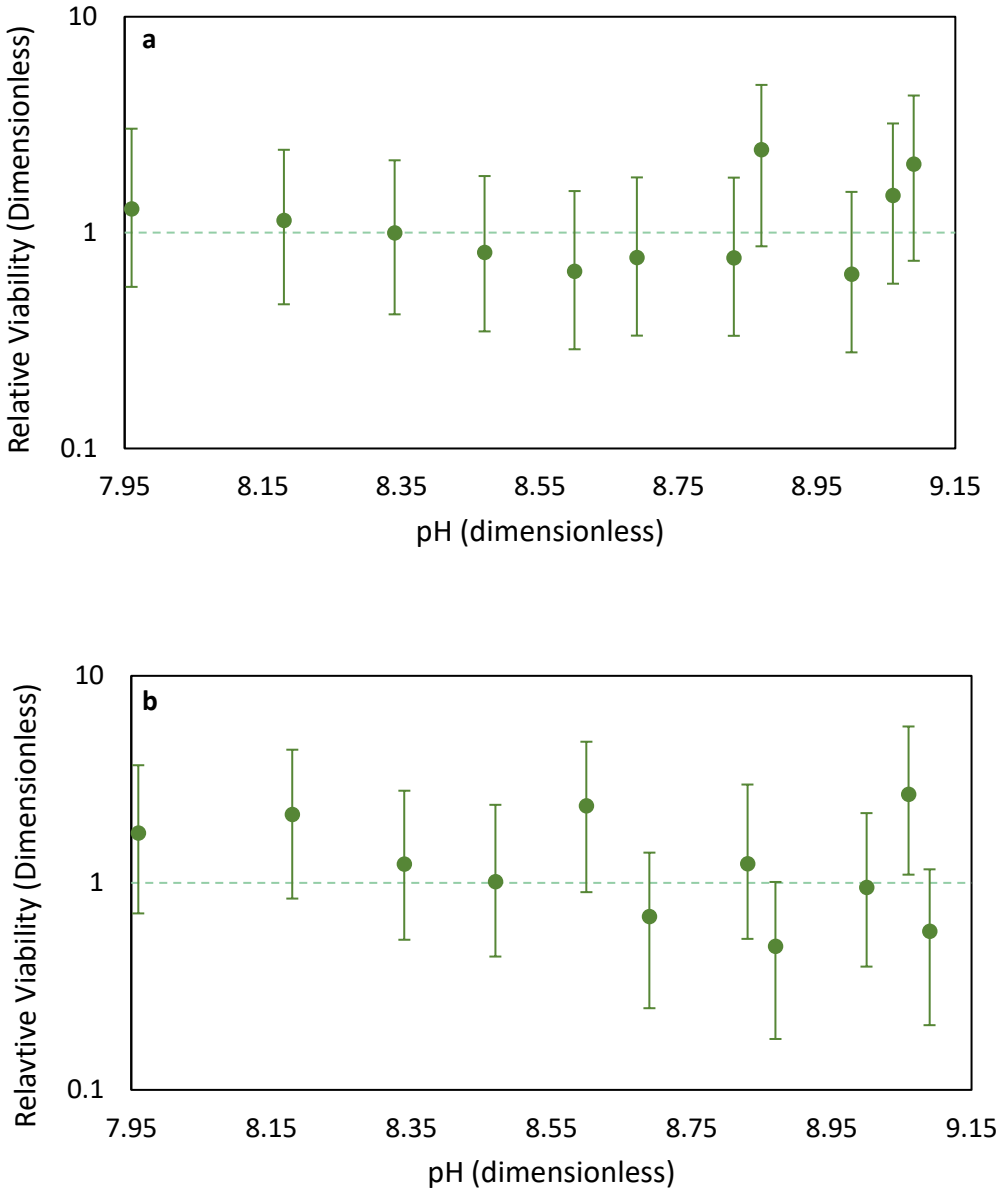

Figure 17: Dose-response curves showing the effect of transient (10-minute) exposure to increasing pH on the relative viability of (a) *Thalassiosira pseudonana* and (b) *Pavlova lutheri*. Error bars are the 95% Confidence Intervals. The dashed line is a Relative Viability of 1 (*i.e.*, no change). As these fall within the 95% CI of all samples, there is no effect of transient pH increases on viability. Regression of Relative Viability on pH was not significant ($p > 0.05$).

In addition to testing for an effect on viability, the physiological indicators of F_v/F_m and μ were examined following transient exposure to elevated pH and alkalinity. Figure 18 shows the impact of elevated pH on F_v/F_m, the proportion of functional PSII reaction centers, measured 1–2 hours following treatment in both *T. pseudonana* and *P. lutheri*. The average F_v/F_m value for *T. pseudonana* is 0.46, and the average value for *P. lutheri* is 0.43. There was no significant trend ($p > 0.05$) in F_v/F_m with pH during exposure for *P. lutheri*, with a linear model. However, there was a significant trend in F_v/F_m with pH for *T. pseudonana*. The data was fit with the biphasic model (Equation 2a and b) and the threshold pH was calculated at 8.86±0.238.

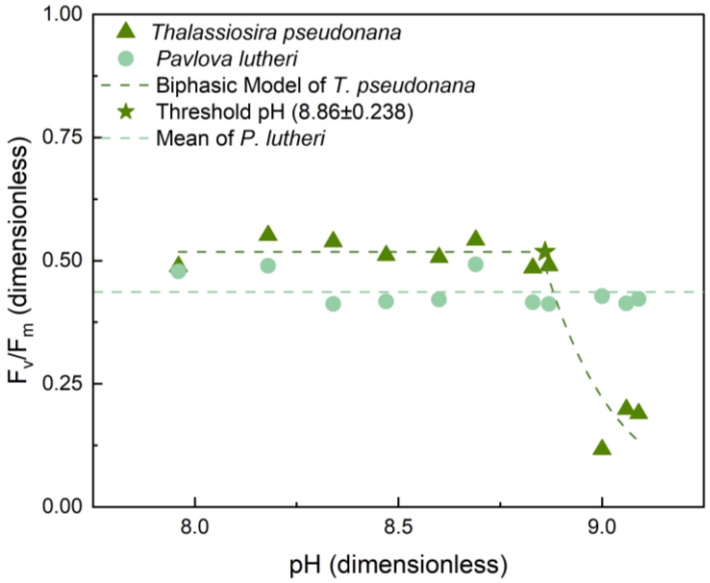

Figure 18: Measurements of F_v/F_m measured after exposure to elevated pH for 1-2 hours in *Thalassiosira pseudonana* and *Pavlova lutheri*. The biphasic model used to fit data for *T. pseudonana* is Equation 2. The estimated threshold pH for reduced F_v/F_m was 8.86±0.24.

Figure 19 shows the impact of transiently elevated pH on μ_m, the maximum (exponential phase) growth rate in both *T. pseudonana* and *P. lutheri*. The 10^{-3} dilution from the SDC–MPN assays was used to calculate the specific growth rate for each treatment from the daily observations of chlorophyll fluorescence (Equations 8 and 9). This dilution tier, in which pH had returned to pre-treatment levels (Figure 16), was used for the comparison because it was the lowest dilution common to all treatments. Neither a linear regression nor the Bannister model gave statistically significant fits to the data ($p < 0.05$): it can be concluded that there is no significant change in the specific growth rate following transient (10-minute) exposure to increasing pH.

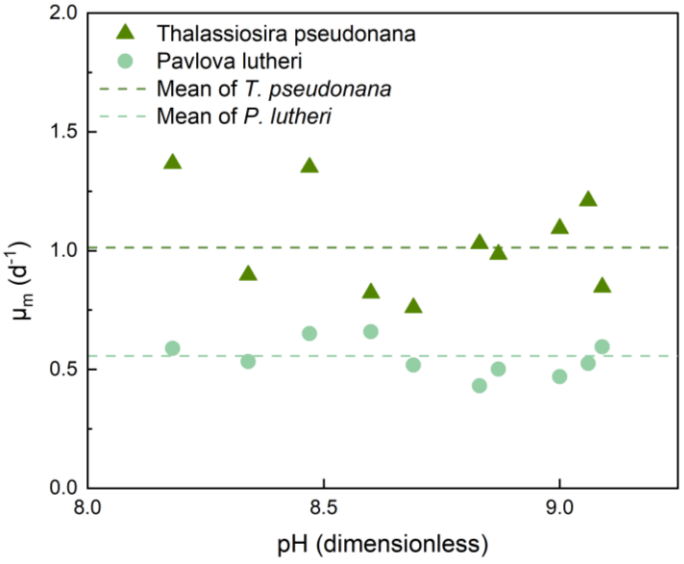

Figure 19: Maximum growth rates (μ_m) as a function of exposure pH during transient exposure in *Thalassiosira pseudonana* and *Pavlova lutheri* for cultures that had been diluted to 10^{-3}. Cultures were exposed to elevated pH for a 10-minute period before being diluted. There was no significant trend in μ_m with pH during the exposure ($p > 0.05$ for linear regression).

4.4.3 Chronic Impacts

The impacts of chronic exposure to elevated pH were examined using F_v/F_m and fluorescence-based estimates of μ_m. Figure 20 shows the average value of F_v/F_m at mid-exponential phase for each pH tested. Mid-exponential was chosen because the cultures had been exposed to the elevated pH for approximately 2 days but were not yet experiencing nutrient limitation during stationary phase that would impact the F_v/F_m value (Kolber et al., 1998). The trends are not significant ($p > 0.05$), based on linear regression.

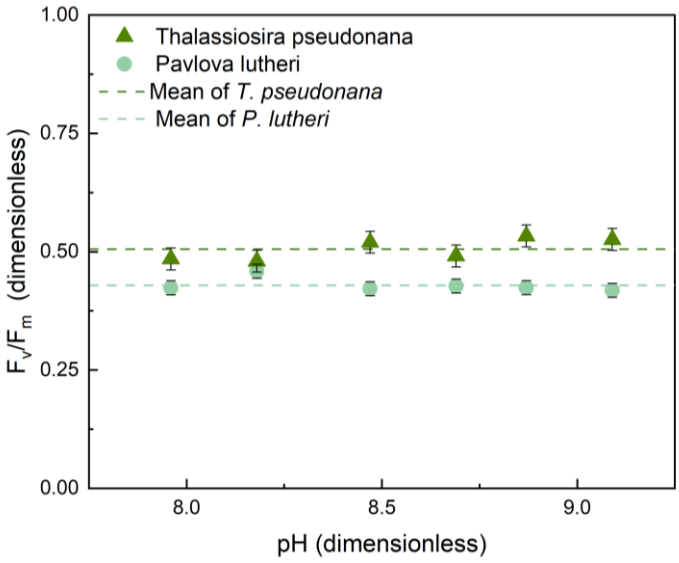

Figure 20: Measurements of F_v/F_m in mid-exponential phase during chronic exposure to elevated pH in *Thalassiosira pseudonana* and *Pavlova lutheri*. There was no significant ($p < 0.05$) trend for either.

Time-course measurements of fluorescence measurements were used to calculate μ_m for each treatment using Equations 8 and 9 are in Figure 21. The cultures were exposed to elevated pH for a period of 8 days and cultured in batch. The pH-dependence was calculated using Equation 2a & c with μ_m (rather than μ) as the dependent variable. In both cases, the fits were

significant ($p < 0.05$). The threshold values of pH above which the exponential growth rate declined were 8.59±0.059 for *T. pseudonana* and 8.68±0.199 for *P. lutheri*. The mean values for diatoms and prynmnesiophytes in pH-drift batch cultures (Figure 6) were 8.58 and 8.78.

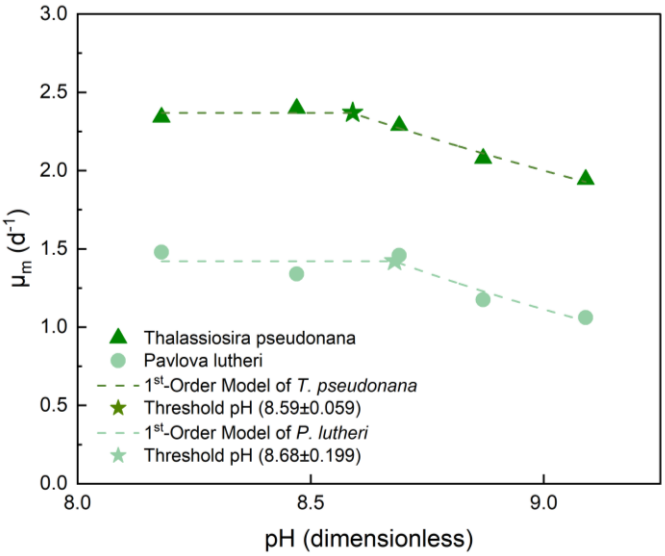

Figure 21: Maximum growth rates (μ_{max}) in *Thalassiosira pseudonana* and *Pavlova lutheri* for cultures that were exposed to elevated pH for an 8-day period. Lines are the fits to Equation 2a and c.

4.5 Discussion

There is no negative impact from elevated pH on *Thalassiosira pseudonana* and *Pavlova lutheri* for the transient exposure cultures, but there is a negative impact for the chronic exposure cultures. For the purposes of this work, a transient exposure is a 10-minute period and chronic is anything longer than 5 hours. The difference in responses is likely due to changes in pH, as discussed in Chapter 2 with the comparison between pH drift and constant pH cultures (Figure 8). A transient exposure is unlikely to change the overall carbon speciation since the

culture would be diluted in 10-minutes and returned to the original pH as in Figure 16, but a chronic exposure could lead to changes in carbon speciation, as in the Bjerrum plot of Figure 1a. When comparing the chronic drift and constant pH experiments in Figure 8 with the transient and chronic experiments in this chapter, it becomes clear that a chronic exposure to highly elevated pH (above c. 8.5) causes a decrease in growth rate for diatoms and prymnesiophytes. This data serves as an indicator of the potential impacts of OAE and gives insight into how phytoplankton would respond and adapt to consistently higher pH and alkalinity than they are accustomed to. Even though chronic exposure is unlikely with timescales of dilution in a real-world scenario, OAE will cause long-term (years) changes to pH that must be understood before implementation. Transient exposure in laboratory tests is also important because it more closely mimics the dissolution of hydroxide and the mixing rate of the receiving waters, predicting how species will respond in the short-term.

All the cultures discussed in this chapter were grown in batch however it is important to discuss the differences between batch and semi-continuous culturing techniques, and why semi-continuous laboratory cultures are better suited for predicting the impacts of OAE. In batch cultures there are three primary growth phases: lag, exponential, and stationary (Gompertz, 1825). The lag phase is generally when the culture is growing slowly and/or growth is below the LLD of the detector used to estimate it, and the exponential phase is the period of most rapid growth. The last phase, stationary, occurs when an essential resource becomes limiting and the growth rate declines to zero. One constraint of batch cultures is that they often self-shade, meaning that as the population grows, the cells growing at the edge of the container are blocking light from cells growing in the middle. Culture cannot be considered as acclimated to an environmental driver due to the constant changes in light and nutrients

(MacIntyre & Cullen, 2005). Semi-continuous culturing is a more controlled approach, in which cells are maintained in exponential growth through regular dilutions. This culturing method removes the confounding variables of nutrient limitation and self-shading (MacIntyre & Cullen, 2005) when investigating why μ decreases with increasing pH. It also more closely resembles the situation in which OAE will be occurring in a natural environment, as diffusion and regular system flushing are likely to be major influences.

The threshold pH values for reductions in growth rate with chronic exposure to high pH were 8.59 and 8.68 for *T. pseudonana* and *P. lutheri*, respectively. These align with the average threshold values observed in Chapter 2 for diatoms (8.23 – 9.56) and prymnesiophytes (8.47 – 8.69) measured in pH-drift experiments. Transient exposure to elevated pH did not have a statistically significant impact on F_v/F_m for *P. lutheri*, however there was a significant reduction in *T. pseudonana* at the highest pH values tested (8.87 – 9.09). Chronic exposure to elevated pH also had no statistical impact on mid-exponential F_v/F_m for either species. This suggests that it takes between 2 hours and several days for F_v/F_m of *T. pseudonana* acclimate to elevated pH. At this pH the dominant carbon species would be carbonate and calcite would begin precipitating, which may account for the reductions in growth rates (Figure 21). Elevating the pH this high is highly undesirable from the perspective of OAE, as calcite precipitation releases CO_2 rather than traps it. It is possible through the accidental discharge of a concentrated hydroxide slurry, so the degree of impairment represents a worst-case scenario.

For a well-rounded understanding of the impacts of OAE on coastal phytoplankton, other species should be examined, such as cryptophytes and *Synechococcus*, both of which are common in Bedford Basin (Robicheau et al., 2022), a coastal embayment and potential trial site for OAE. Cryptophytes are commonly found in Bedford Basin when nutrients are high and

temperatures are low (Robicheau et al., 2022), and *Synechococcus* generally dominates during the late summer (Li & Dickie, 2001). Understanding how these species of phytoplankton, in addition to *T. pseudonana* and *P. lutheri*, respond to transient and chronic exposures to pH would create a more holistic view of the possible response to OAE. All cultures examined in Chapter 2 and 4 were monocultures, containing only one strain of phytoplankton, but the relationship in a natural environment is complex. While one species may be able to survive, if not thrive, under elevated pH conditions, others may be negatively impacted. This would then alter the population dynamics and could impact the trophic systems. Testing possible impacts on coastal assemblages, under realistic conditions of concentration and duration of exposure to elevated pH, is vital before OAE can be implemented.

4.6 Conclusions

The overarching conclusion that can be drawn from the data is that there is no change in growth rates or viability when the studied phytoplankton species are transiently exposed to increases in pH, although there may be a transient depression in F_v/F_m at very high pH. There are significant changes in growth rates with chronic exposure to elevated pH that are consistent with reports from the literature. This suggests that the available literature on responses to elevated pH, which is all based on chronic exposure in pH-drift or semi-continuous culture, is likely to overestimate the potential impact of OAE if the hydroxide is diluted on time-scales of 10 minutes to 1-2 hours following discharge into the receiving waters.

CHAPTER 5

CONCLUSIONS

The pressing problem of climate change remains one of the most critical issues that must be resolved in the coming decades, and one of the only ways to achieve this is through actively removing carbon from the atmosphere. Sequestering carbon for long timescales has proven to be a significant challenge, but OAE could be a solution by simply enhancing the ocean's natural alkalinity cycle (Minx et al., 2018). The results of this study aid in exploring the possible impacts of OAE on the biological environment, specifically phytoplankton.

The literature is mined in Chapter 2 of this thesis to assess how pH, and subsequently potential OAE, would impact a large range of taxonomic species. The most significant conclusion is that the increase in pH from OAE is below the average threshold dose for all taxonomic groups investigated to date. Variability within taxonomic groups is most likely caused by differences in CCMs, Rubisco type, or sensitivity to elevated internal pH; however, the majority of phytoplankton studied would be unaffected by OAE at the pHs most effective at trapping CO_2 in bicarbonate (6 – 9; see Figure 1a).

A modified method for the SDC–MPN assay using polystyrene cell culture plates was validated against the test conducted in borosilicate glass tubes in Chapter 3. By following the strong inference method from Platt (1964) it was determined that selenium must be added to f/2 growth media (Guillard, 1975) for phytoplankton to grow successfully in plasticware. The second growth medium used, L1 (Guillard & Hargraves, 1993) already contains selenium and did not require further modification. This provided support for using the assay in Chapter 4.

The focus for the final chapter was testing for effects of transient and chronic exposure to elevated pH in *T. pseudonana* and *P. lutheri*. Ultimately, there was no impact from transient exposure (10 minutes to 2 hours) on viability or μ at the pHs tested for both species, but there was an impact on F_v/F_m for *T. pseudonana* at high pH (8.87 – 9.09). However, when the same species experienced chronic exposure to elevated pH a threshold value was observed in μ, consistent with the values previously observed in pH-drift cultures, but there was no significant change in F_v/F_m for either species.

With an understanding of the relationship between elevated pH and the impact on phytoplankton growth established from Chapter 2, and the comparison between short- and long-term exposure to elevated pH in *T. pseudonana* and *P. lutheri* in Chapter 4, it can be concluded that there will likely be little to no impact from OAE on the two species of phytoplankton studied. Future work examining the impacts of OAE on phytoplankton should focus on the potential changes to community dynamics and further investigate the influence on photosynthetic competence. Trophic cascades could result from the removal of a single species of phytoplankton if they are unable to tolerate changes from OAE, or the removal of grazers unable to withstand OAE could allow for phytoplankton species to overpopulate and cause harmful algae blooms. Additionally, the phenomenon observed in *T. pseudonana* of a decrease in F_v/F_m after transient exposure compared to no impact in the chronic exposure culture needs to be investigated further. Determining if this response is a widespread occurrence in all diatoms, or if other aspects of photosynthesis are affected will be important for the successful implementation of OAE.

Overall, while further work is needed to thoroughly investigate the rate of diffusion and mixing at a release site, as well as possible impacts to phytoplankton community dynamics, these preliminary findings are positive indicators for successful implementation.

APPENDIX A

CHAPTER 4

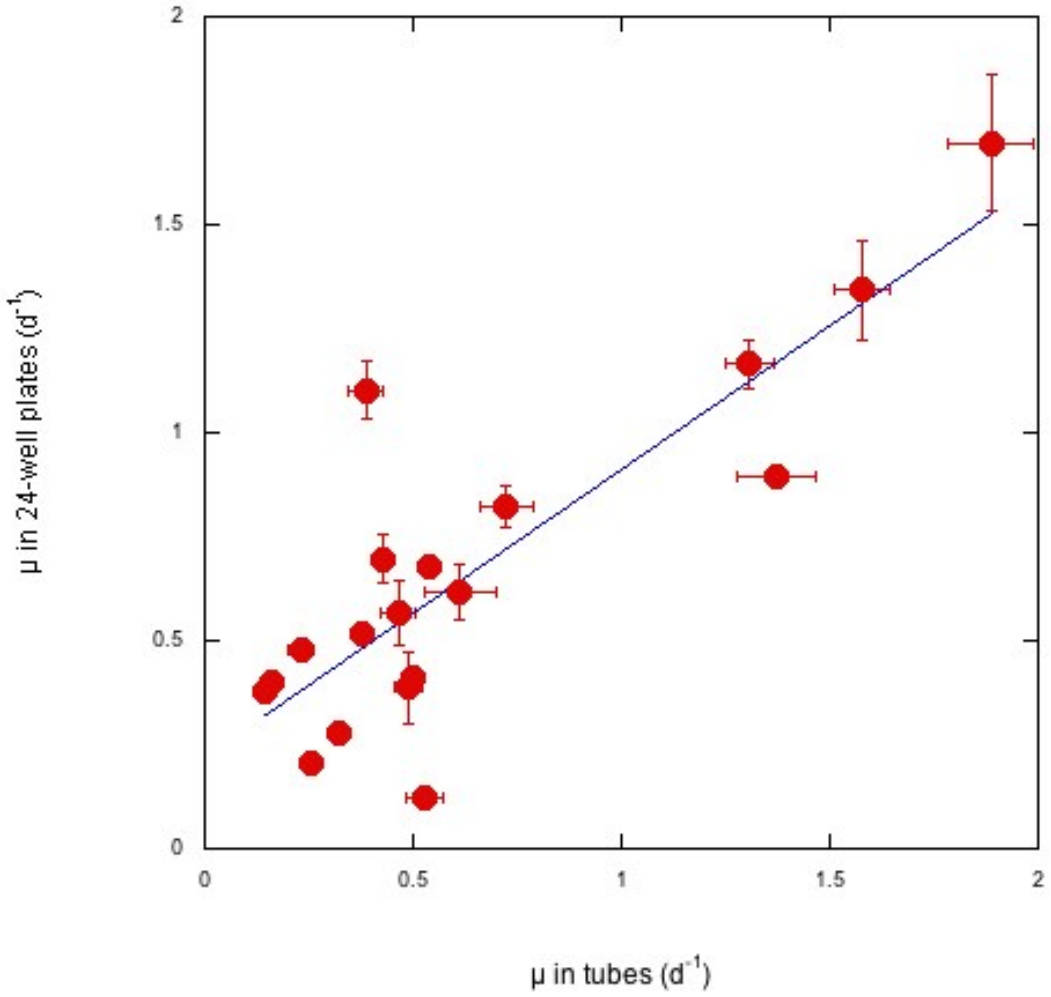

Figure A.1: Comparison of growth rates (μ) in 24-well plates and borosilicate glass tubes. Cultures grown at low irradiance (20 μmol photons m^{-2}) tend to grow faster in plates (left side of graph), and cultures grown at high irradiance (190 μmol photons m^{-2}) tend to grow slower in plates (right side of graph). (MacIntyre et al., in prep)

Table A.1: Descriptions of all articles used for digitization in Chapter 2.

Primary Author	Year	Species	Strain	Isolation place	Isolation Year	Taxonomic Group	Media type	Photoperiod	Irradiance	Temperature
Hansen, P. J.	2002	*Ceratium lineatum*	N/A	Øresund, Denmark	1995	Dinoflagellate	f/2	16h:8h	60 µmol photons	15 ±1°C
		Heterocapsa triquetra	K-0481	Øresund, Denmark	1988	Dinoflagellate				
		Prorocentrum minimum	K-0295	Kattegat, Denmark	1989	Dinoflagellate				
Lundholm, N.	2004	*Pseudo-nitzschia pungens*	CL-193	Deadmans Harbour, Bay of Fundy, Canada	2002	Diatom	L1	16h:8h	100 µmol photons	15 ±1°C
		Pseudo-nitzschia multiseries	CL-195	Deadmans Harbour, Bay of Fundy, Canada	2002	Diatom				
		Pseudo-nitzschia multiseries	OKPm013-2	Okkiray Bay, Iwate Prefecture, Japan	2001	Diatom				
		Nitzschia navis-varingica	VHL987	Ha Long Bay, Vietnam	1998	Diatom				
		Pseudo-nitzschia australis	PS11V	Baiona, Ría Vigo, Spain	2001	Diatom				
		Pseudo-nitzschia sp.	NWFSC095	Sequim Bay, Washington, USA	2002	Diatom				

Primary Author	Year	Species	Strain	Isolation place	Isolation Year	Taxonomic Group	Media type	Photoperiod	Irradiance	Temperature
Lundholm, N.	2004	*Pseudo-nitzschia calliantha*	CL-190	Baie-Sainte-Anne, New Brunswick, Canada	2002	Diatom	L1	16h:8h	100 µmol photons	15 ±1°C
		Pseudo-nitzschia delicatissima	Tasm10	Hobart Harbour, Tasmania	2000	Diatom				
		Pseudo-nitzschia fraudulenta	CL-192	Deadmans Harbour, Bay of Fundy, Canada	2002	Diatom				
		Pseudo-nitzschia granii	PG	Ocean Station Papa, NE Pacific	2000	Diatom				
		Pseudo-nitzschia seriata	CL-150	Tracadie Harbour, PEI, Canada	2002	Diatom			55 µmol photons	4°C
		Pseudo-nitzschia cf. turgidula	PT	Ocean Station Papa, NE Pacific	2002	Diatom			100 µmol photons	15 ±1°C
Hansen, P. J	2007	*Ceratium lineatum*	N/A	Øresund, Denmark	1995	Dinoflagellate	f/2	16h:8h	60 µmol photons	15 ±1°C
		Heterocapsa triquetra	K-0481	Øresund, Denmark	1988	Dinoflagellate				
		Prorocentrum minimum	K-0295	Kattegat, Denmark	1989	Dinoflagellate				
Schmidt, L. E.	2001	*Chrysochromulina polylepis*	K-0259	Øresund, Denmark	1988	Prymnesiophyte	f/2	16h:8h	60 µmol photons	15 ±1°C
		Chrysochromulina simplex	K-0272	Victoria, Austalia	1988	Prymnesiophyte				

Primary Author	Year	Species	Strain	Isolation place	Isolation Year	Taxonomic Group	Media type	Photoperiod	Irradiance	Temperature
Møgelhøj, M. K.	2006	*Rhodomonas marina*	K-0435	Kattegat, Denmark	1990	Cryptophyte	B1 modified using 0.5 mL vitamin stock/L	16h:8h	65 µmol photons	15 ±2°C
		Rhodomonas salina	K-0294	Øresund, Denmark	1989	Cryptophyte				
		Heterocapsa triquetra	K-0481	Øresund, Denmark	1988	Dinoflagellate				
		Prorocentrum micans	K-0335	Kattegat, Denmark	1989	Dinoflagellate				
		Prorocentrum minimum	K-0295	Kattegat, Denmark	1989	Dinoflagellate				
		Phaeodactylum tricornutum	N/A	Unknown	Unknown	Diatom				
Nielsen, L. T.	2007	*Heterocapsa triquetra*	N/A	Unknown	Unknown	Dinoflagellate	f/2 w/ 3x Si	16h:8h	20, 35, 80, and 250 µmol photons	16.5 ±0.5°C
		Nitzschia navis-varingica	VHL985	Unknown	Unknown	Diatom				
Berge, T	2010	*Prorocentrum minimum*	K-1138	Skagerrak	2008	Dinoflagellate	f/2	14h:10h	150 µmol photons	15°C
		Prorocentrum micans	K-1137	Skagerrak	2008	Dinoflagellate				
		Karlodinium veneficum	K-1413	North Sea	2007	Dinoflagellate				
		Heterocapsa triquetra	K-1133	Baltic	2007	Dinoflagellate				
		Rhodomonas marina	K-0435	Kattegat, Denmark	1990	Cryptophyte				
		Teleaulax amphioxeia	N/A	The Sound, Denmark	2009	Cryptophyte				
		Coscinodiscus granii	K-1048	USA	1994	Diatom				
		Prymnesium parvum	K-0623	Unknown	Unknown	Prymnesiophyte				

Primary Author	Year	Species	Strain	Isolation place	Isolation Year	Taxonomic Group	Media type	Photoperiod	Irradiance	Temperature
Berge, T	2012	*Heterocapsa triquetra*	A4c, NA	Copenhagen, Denmark	2007	Dinoflagellate	L1	16h:8h	150 µmol photons	15°C
		Heterocapsa triquetra	A5c, K-1134	Copenhagen, Denmark	2007	Dinoflagellate				
		Heterocapsa triquetra	A2b, K-1131	Copenhagen, Denmark	2007	Dinoflagellate				
		Heterocapsa triquetra	A4a, Na	Copenhagen, Denmark	2007	Dinoflagellate				
		Heterocapsa triquetra	F2e, NA	Gedser Harbour, Denmark	2007	Dinoflagellate				
		Heterocapsa triquetra	F1f, NA	Gedser Harbour, Denmark	2007	Dinoflagellate				
		Heterocapsa triquetra	F1c, K-1125	Gedser Harbour, Denmark	2007	Dinoflagellate				
		Heterocapsa triquetra	F1a, K-1124	Gedser Harbour, Denmark	2007	Dinoflagellate				
		Heterocapsa triquetra	2-1, K-1127	Stege Harbour, Denmark	2007	Dinoflagellate				
		Heterocapsa triquetra	2-3, NA	Stege Harbour, Denmark	2007	Dinoflagellate				
		Heterocapsa triquetra	2-5, NA	Stege Harbour, Denmark	2007	Dinoflagellate				
		Heterocapsa triquetra	2-6, NA	Stege Harbour, Denmark	2007	Dinoflagellate				
		Heterocapsa triquetra	HTMS0402	Masan Bay Korea	2004	Dinoflagellate				

Primary Author	Year	Species	Strain	Isolation place	Isolation Year	Taxonomic Group	Media type	Photoperiod	Irradiance	Temperature
Berge, T	2012	*Heterocapsa triquetra*	KAC 26	Kalmarsund, Sweden	2000	Dinoflagellate	L1	16h:8h	150 µmol photons	15°C
		Heterocapsa triquetra	KAC 27	Kalmarsund, Sweden	2000	Dinoflagellate				
		Heterocapsa triquetra	NC 98	West Coast, Norway	1998	Dinoflagellate				
		Heterocapsa triquetra	K-0482	Kattegat, Denmark	1988	Dinoflagellate				
		Heterocapsa triquetra	KAC 49	West Coast, Sweden	1986	Dinoflagellate				
		Heterocapsa triquetra	K-0447	The Sound, Denmark	1984	Dinoflagellate				
		Heterocapsa triquetra	NIES 235	Osaka Bay, Japan	1982	Dinoflagellate				
		Heterocapsa triquetra	NIES 7	Farima-Nada, Japan	1981	Dinoflagellate				
		Heterocapsa triquetra	CCMP 449	Lawrence Estuary, Canada	1960	Dinoflagellate				
		Heterocapsa triquetra	PLY 169	Tamar Estuary, England	1957	Dinoflagellate				
Søgaard, D. H.	2011	Fragilariopsis sp.	CCMP 2297	Baffin Bay	1998	Diatom	L1	16h:8h	50 µmol photons	3 ±2°C
		Chlamydomonas sp.	CCMP 2294	Baffin Bay	2003	Chlorophyte				
		Fragilariopsis nana	SCCAP K-0637	Labrador Sea	Unknown	Diatom				

Primary Author	Year	Species	Strain	Isolation place	Isolation Year	Taxonomic Group	Media type	Photoperiod	Irradiance	Temperature
Søderberg, L. M.	2007	*Ceratium fusus*	N/A	The Sound, Denmark	2003	Dinoflagellate	f/2	16h:8h	100 µmol photons; 25 & 200 µmol photons	15 ±1°C
		Ceratium furca	N/A	The Sound, Denmark	2003	Dinoflagellate				
		Ceratium tripos	N/A	The Sound, Denmark	1998	Dinoflagellate				
Weisse, T.	2006	*Cryptomonas sp.*	SAG 26.80	Unknown	Unknown	Cryptophyte	MWC	14h:10h	10-30 µmol photons	15 ±0.2°C
Liu, W.	2007	*Chattonella marina*	NIES-3	Osaka Bay, Japan	1982	Raphidophyte	K	12h:12h	c. 42 µmol photons	22-24°C

REFERENCES

Albrecht M, Khanipour Roshan S, Fuchs L, Karsten U, Schumann R. (2022). Applicability and limitations of high-throughput algal growth rate measurements using in vivo fluorescence in microtiter plates. *J Appl Phycol.* 34 (4):2037-2049.

Allen EH. (1919). A contribution to the quantitative study of phytoplankton. *Journal of the Marine Biological Association of the United Kingdom*. 12(1): 1-8.

Bannister TT. (1979). Quantitative description of steady state, nutrient-saturated algal growth, including adaptation. Limnol. Oceanogr. 24: 76-96.

Bannon CC & Campbell DA. (2017). Sinking towards destiny: High throughput measurements of phytoplankton sinking rates through time-resolved fluorescence plate spectroscopy. *PLoS ONE*, 12(10).

Badger MR, Andrews TJ, Whitney SM, Ludwig M, Yellowlees DC, Leggat W, & Price GD. (1998). The diversity and coevolution of Rubisco, plastids, pyrenoids, and chloroplast-based CO_2 -concentrating mechanisms in algae. *Canadian Journal of Botany*, *76*(6), 1052–1071. https://doi.org/10.1139/b98-074

Badger MR & Bek EJ. (2008). Multiple Rubisco forms in proteobacteria: their functional significance in relation to CO2 acquisition by the CBB cycle. J. Exp. Bot. 59: 1525–1541.

Berge T, Daugbjerg N, Balling Andersen B, & Hansen PJ. (2010). Effect of lowered pH on marine phytoplankton growth rates. *Marine Ecology Progress Series*, *416*, 79–91. https://doi.org/10.3354/meps08780

Berge T, Daugbjerg N, & Hansen PJ. (2012). Isolation and cultivation of microalgae select for low growth rate and tolerance to high pH. *Harmful Algae*, *20*, 101–110. https://doi.org/10.1016/j.hal.2012.08.006

Blackman, FF. (1905). Optima and limiting factors. Ann. Bot. 19:281.295.

Blatchley III ER, Cullen JJ, Petri B, Bircher K, & Welschmeyer N. (2018). The Biological Basis for Ballast Water Performance Standards: "Viable/Non-Viable" or "Live/Dead"? *Environmental Science & Technology*, *52*(15), 8075–8086. https://doi.org/10.1021/acs.est.8b00341

Castaldello C, Gubert A, Sforza E, Facco P, Bezzo F. (2021). Microalgae Monitoring in Microscale Photobioreactors via Multivariate Image Analysis. *ChemEngineering.* 5 (3):49

Cochran WG. (1950). Estimation of bacterial densities by means of most probable number. Biometrics. 6:105-116.

Colman B, Huertas IE, Bhatti S, & Dason JS. (2002). The diversity of inorganic carbon acquisition mechanisms in eukaryotic microalgae. *Functional Plant Biology*, *29*(3), 261. https://doi.org/10.1071/PP01184

Cullen JJ & MacIntyre HL. (2016). On the use of the serial dilution culture method to enumerate viable phytoplankton in natural communities of plankton subjected to ballast water treatment. *Journal of Applied Phycology*, *28*(1), 279–298. https://doi.org/10.1007/s10811-015-0601-x

Dlugokencky E. & Tans P. (2018). Trends in atmospheric carbon dioxide, National OCeanic & Atmospheric Administration. *Earth System research Laboratory (NOAA/ERSL)*.

Flowers P, Theopold P, Langely R & Robinson WR. (2019). Chapter 14 Acid-Base Equilibria. In *Chemistry 2E*. essay, OpenStax. Retrieved 2022, from https://openstax.org/books/chemistry-2e/pages/14-introduction

Ghorbani Y, Franzidis J-P & Petersen J. (2015). Heap leaching technology – current state, innovations and future directions: A review. *Mineral Processing and Extractive Metallurgy Review*, 08827508.2015.1115990. https://doi.org/10.1080/08827508.2015.1115990

Galland G, Harrould-Kolieb E, & Herr D. (2012). The ocean and climate change policy. *Climate Policy*, *12*(6), 764–771. https://doi.org/10.1080/14693062.2012.692207

Gattuso J-P. (2018). Ocean Solutions to Address Climate Change and Its Effects on Marine Ecosystems. *Frontiers in Marine Science*, *5*, 18.

Gompertz B (1825) XXIV. On the nature of the function expressive of the law of human mortality, and on a new mode of determining the value of life contingencies. In a letter to Francis Baily, Esq. F. R. S. &c. Philosophical Transactions of the Royal Society of London 115:513-583. doi:10.1098/rstl.1825.0026

Guillard RRL. (1975). Culture of phytoplankton for feeding marine invertebrates. In: Smith WL, Chanley MH (eds) Culture of marine invertebrate animals. Plenum, New York, pp 108–132

Guillard RRL, & Hargraves PE. (1993) Stichochrysis immobilis is a diatom, not a chrysophyte. Phycologia 32:234–236

Haas CN, & Heller B. (1988). Test of the validity of the Poisson assumption for analysis of most-probable-number results. Appl Envrion Microbial. 54:2996-3002

Hansen PJ. (2002). Effect of high pH on the growth and survival of marine phytoplankton: Implications for species succession. *Aquatic Microbial Ecology*, *28*, 279–288. https://doi.org/10.3354/ame028279

Hansen PJ, Lundholm N, & Rost B. (2007). Growth limitation in marine red-tide dinoflagellates: Effects of pH versus inorganic carbon availability. *Marine Ecology Progress Series*, *334*, 63–71. https://doi.org/10.3354/meps334063

Hijnen WAM, Beerendonk EF, Medema GJ (2006) Inactivation credit of UV radiation for viruses, bacteria and protozoan (oo)cysts in water: A review. Water Res 40 (1):3-22. doi:10.1016/j.watres.2005.10.030

Hofmann GE, Smith JE, Johnson KS, Send U, Levin LA, et al. (2011). High-Frequency Dynamics of Ocean pH: A Multi-Ecosystem Comparison. PLoS ONE 6(12): e28983.

Iñiguez C, Capó-Bauçà S, Niinemets Ü, Stoll H, Aguiló-Nicolau P, Galmés J (2020) Evolutionary trends in RuBisCO kinetics and their co-evolution with CO2 concentrating mechanisms. Plant J 101 (4):897-918. doi:https://doi.org/10.1111/tpj.14643

IPCC, Global warming of 1.5°C. An IPCC Special Report on the impacts of global warming of 1.5°C above pre-industrial levels and related global greenhouse gas emission pathways, in the context of strengthening the global response to the threat of climate change, sustainable development, and efforts to eradicate poverty, V. Masson-Delmotte, et al., Editors. 2018, World Meteorological Organization: Geneva, Switzerland. p. 32.

Jones CT, Craig SE, Barnett AB, MacIntyre HL, Cullen JJ (2014) Curvature in models of the photosynthesis-irradiance response. J Phycol 50 (2):341-355. doi:10.1111/jpy.12164

Jordan DB & Ogren WL. (1981). Species variation in the specificity of ribulose bisphosphate carboxylase/oxygenase. Nature. 291: 513–515.

Keller DP, Lenton A, Littleton EW, Oschlies A, Scott V & Vaughan NE. (2018). The Effects of Carbon Dioxide Removal on the Carbon Cycle. *Current Climate Change Reports*, *4*(3), 250–265.

Kolber Z, Zehr J, Falkowski P (1988) Effects of growth irradiance and nitrogen limitation on photosynthetic energy conversion in photosystem II. Plant Physiol 88:923-929

Lenton A, Matear RJ, Keller DP, Scott V & Vaughan NE. (2018). Assessing carbon dioxide removal through global and regional ocean alkalinization under high and low emission pathways. *Earth System Dynamics*, *9*(2), 339–357.

Li WKW & Dickie PM. (2001). Monitoring phytoplankton, bacterioplankton, and virioplankton in a coastal inlet (Bedford Basin) by flow cytometry. *Cytometry*, *44*(3), 236–246.

Li WKW & Harrison GW. (2008). Propagation of an atmospheric climate signal to phytoplankton in a small marine basin. Limnol. Oceanogr. 53(3):1734-1745.

Liu W, Au DWT, Anderson DM, Lam PKS, & Wu RSS. (2007). Effects of nutrients, salinity, pH and light:dark cycle on the production of reactive oxygen species in the alga Chattonella marina. *Journal of Experimental Marine Biology and Ecology*, *346*(1–2), 76–86. https://doi.org/10.1016/j.jembe.2007.03.007

Lundholm N, Hansen PJ, & Kotaki Y. (2004). Effect of pH on growth and domoic acid production by potentially toxic diatoms of the genera *Pseudo-nitzschia* and *Nitzschia*. Mar. Ecol. Prog. 273, 1-15.

MacIntyre HL & Cullen JJ (2005). Using Cultures to Investigate the Physiological Ecology of Microalgae. In *Algal Culturing Techniques* (pp. 287–326). Elsevier. https://doi.org/10.1016/B978-012088426-1/50020-2

MacIntyre HL, Cullen JJ, Whitsitt TJ, & Petri B. (2018). Enumerating viable phytoplankton using a culture-based Most Probable Number assay following ultraviolet-C treatment. *Journal of Applied Phycology*, *30*(2), 1073–1094. https://doi.org/10.1007/s10811-017-1254-8

MacIntyre HL, Cullen JJ, Rastin S, Waclawik M, Franklin KJ, Poulton N, Lubelczyk L, McPhee K, Richardson TL, Van Meerssche E, & Petri B. (2019). Inter-laboratory validation of the serial dilution culture—Most probable number method for enumerating viable phytoplankton. *Journal of Applied Phycology*, *31*(1), 491–503. https://doi.org/10.1007/s10811-018-1541-z

Magnan AK, Billé R, Bopp L, Chalastani VI, Cheung WWL, Duarte CM, Gates RD, Hinkel J, Middelburg JJ, & Oschlies A. (2018). *Ocean-based measures for climate action*. 5.

Margalef R. (1978). Life-forms of phytoplankton as survival alternatives in an unstable environment. *Oceanol. Acta*, 1(4), 493-509.

McCrady MH (1915). The numerical interpretation of fermentation-tube results. J Infect Dis. 17:183-212.

Minx JC, Lamb WF, Callaghan MW, Fuss S, Hilaire J, Creutzig F, Amann T, Beringer T, de Oliveira Garcia W, Hartmann J, Khanna T, Lenzi D, Luderer G, Nemet GF, Rogelj J, Smith P, Vicente JL, Wilcox J, & del Mar Zamora Dominguez M. (2018). Negative emissions—Part 1: Research landscape and synthesis. *Environmental Research Letters*, *13*(6), 063001. https://doi.org/10.1088/1748-9326/aabf9b

Møgelhøj M, Hansen PJ, Henriksen P, & Lundholm N. (2006). High pH and not allelopathy may be responsible for negative effects of Nodularia spumigena on other algae. *Aquatic Microbial Ecology*, *43*, 43–54. https://doi.org/10.3354/ame043043

Nielsen LT, Lundholm N, & Hansen PJ. (2007). Does irradiance influence the tolerance of marine phytoplankton to high pH? Mar. Bio. Res. 3(6), 446-453

Nimer NA, Iglesias-Rodriguez MD, Merrett MJ. (1997). Bicarbonate utilization by marine phytoplankton species. J Phycol. 33:625–631

NOAA National Estuarine Research Reserve System (NERRS). System-wide Monitoring Program. Data accessed from the NOAA NERRS Centralized Data Management Office website: http://www.nerrsdata.org; *accessed* 20 October 2022.

O'Brien TD. (2014). *COPEPOD: The Global Plankton Database*. An overview of the 2014 database contents, processing methods, and access interface. U.S. Dep. Commerce, NOAA Tech. Memo. NMFS-F/ST-37, 29p.

Paris Agreement [Treaty No. XXVII-7-d]. (2015). UN Treaty. United Nations.

Pedersen F, & Hansen PJ. (2003). Effects of high pH on a natural marine planktonic community. *Marine Ecology Progress Series*. 260, 19–31. https://doi.org/10.3354/meps260019

Pedersen F, & Hansen PJ. (2003). Effect of high pH on the growth and survival of six marine heterotrophic protists. *Marine Ecology Progress Series*. 260, 33-41.

www.planetarytech.com/technology/. Accessed on September 19, 2022.

Platt JR. (1964). Strong Inference: Certain systematic methods of scientific thinking may produce much more rapid progress than others. *Science*. 146(3642), 347-353.

Price NM, Thompson PA, & Harrison PJ. (1987). Selenium: An essential element for growth of the coastal marine diatom *Thalassiosira pseudonana* (Bacillariophyceae). J. Phycol. 23, 1-9.

Rau GH, Willauer HD, & Ren ZJ. (2018). The global potential for converting renewable electricity to negative-CO2-emissions hydrogen. *Nature Climate Change*, *8*(7), 621–625. https://doi.org/10.1038/s41558-018-0203-0

Raven JA, Beardall J, & Giordano M. (2014). Energy costs of carbon dioxide concentrating mechanisms in aquatic organisms. *Photosynthesis Research*, *121*(2–3), 111–124. https://doi.org/10.1007/s11120-013-9962-7

Raven JA, Beardall J, & Sánchez-Baracaldo P. (2017). The possible evolution and future of CO2-concentrating mechanisms. *Journal of Experimental Botany*, *68*(14), 3701–3716. https://doi.org/10.1093/jxb/erx110

Renforth P, & Henderson G. (2017). Assessing ocean alkalinity for carbon sequestration: Ocean Alkalinity for C Sequestration. *Reviews of Geophysics*, *55*(3), 636–674. https://doi.org/10.1002/2016RG000533

Robicheau BM, Tolman J, Bertrand EM, & LaRoche J. (2022). Highly-resolved interannual phytoplankton community dynamics of the coastal Northwest Atlantic. *ISME Communications*, *2*(1), 38.

Scalet BM, Slade S, Kasper A, de Lummen G.V, Gitzhofer K, & Limpt H. (2006). Selenium emissions from glass melting furnaces: formation, sampling and analysis. Glass Technol.: Eur. J. Glass Sci. Technol. 47(2):29-38.

Schmidt LE & Hansen PJ. (2001). Allelopathy in the prymnesiophyte Chrysochromulina polylepis: effect of cell concentration, growth phase and pH. Mar Ecol Prog Ser. 216:67–81.

Shih PM, Occhialini A, Cameron JC, Andralojc PJ, Parry MA & Kerfeld CA. (2016). Biochemical characterization of predicted Precambrian RuBisCO. Nature Communications 7, 10382.

Søderberg L & Hansen P. (2007). Growth limitation due to high pH and low inorganic carbon concentrations in temperate species of the dinoflagellate genus Ceratium. *Marine Ecology Progress Series*, *351*, 103–112. https://doi.org/10.3354/meps07146

Søgaard DH, Hansen PJ, Rysgaard S, & Glud RN (2011). Growth limitation of three Arctic sea ice algal species: Effects of salinity, pH, and inorganic carbon availability. *Polar Biology*, *34*(8), 1157–1165. https://doi.org/10.1007/s00300-011-0976-3

Stoecker DK. (1999). Mixotrophy among Dinoflagellates. *The Journal of Eukaryotic Microbiology*, *46*(4), 397–401. https://doi.org/10.1111/j.1550-7408.1999.tb04619.x

Tcherkez GGB, Farquahar GD & Andrews TJ. (2006). Despite slow catalysis and confused substrate specificities, all ribulose bisphosphate carboxylases may be nearly perfectly optimized. Proceedings of the National Academy of Sciences, USA 103, 7246–7251

Throndsen J. (1978). The dilution-culture method. In: Sournia A (ed) Phytoplankton Manual. UNESCO, Paris, 218-224.

UNESCO. (2011). *The Impact of Global Change on Water Resources: The Response of UNESCO's International Hydrology Programme.* United Nations Educational Scientific and Cultural Organization (UNESCO) International Hydrological Programme (IHP), Paris, France, 20 pp.

USEPA. (2010). Generic protocol for the verification of ballast water treatment technology., vol Version 5.1. EPA/600/R-10/146. US Environmental Protection Agency Environmental Technology Verification Program, Washington, D.C.

Weavers LK & Wickramanayake GB. (2001). Kinetics of the inactivation of microorganisms. In: Block SS (ed) Disinfection, Sterilization, and Preservation. 5th edn. Lippincott Williams & Wilkins, Philadelphia, PA, pp 65-78

Weisse T & Stadler P. (2006). Effect of pH on growth, cell volume, and production of freshwater ciliates, and implications for their distribution. *Limnology and Oceanography*, *51*(4), 1708–1715. https://doi.org/10.4319/lo.2006.51.4.1708

Winder M, & Sommer U. (2012). Phytoplankton response to a changing climate. *Hydrobiologia*, *698*(1), 5–16.

Wood MA, Everroad RC, Wingard LM (2005) Measuring growth rates in microalgal cultures. In: Andersen RA (ed) Algal Culture Techniques. Academic Press, New York, pp 269-285

Zeng H. (2009). Selenium as an essential micronutrient: roles in cell cycle and apoptosis. Molecules. 14(3):1263-78.

Zhong W & Haigh JD. (2013). The greenhouse effect and carbon dioxide. *Weather*, *68*(4), 100–105. https://doi.org/10.1002/wea.2072

Zwietering MH, Jongenburger I, Rombouts FM, Vantriet K. (1990). Modeling of the bacterial growth curve. Appl Environ Microbiol. 56(6):1875-1881.